Microphysical variability of Amazonian deep convective cores observed by CloudSat and simulated by a multi-scale modeling framework

J. Brant Dodson, Patrick C. Taylor, and Mark Branson

Author Response on ACPD paper acp-2017-864:

Thanks to the anonymous referees and editors for reviewing the manuscript. The main changes to the manuscript include a new figure that illustrates the double-arc feature in the CFAD, the inclusion of SPV4 results both with and without diagnosed graupel, and improvements to the writing of the modeling section in order to better mesh the model results with the observations. The point-by-point responses to the referees are found immediately below. Referee comments are displayed in plain text, and responses are shown in italics with indentation. After that is the revised document with tracked changes.

Anonymous Referee #1

Summary:

The authors use the Amazon as a testbed for assessing the internal structure of deep convection observed by CloudSat. Deep convective cores are shown, through a "double arc" structure in CFADS, to be composed of either highly reflective graupel and hail or weakly reflective snow. Cloud structure is contrasted between day/night and wet season/dry season to modest effect. The authors then compare their CloudSat results with those from two SP-CAM runs. These simulations are conducted with different versions of the model which results in the simulations of differing cloud structure between the simulations themselves and between the simulations and CloudSat. The authors report new results, but these are incremental. There are several aspects of the paper that need improvement: 1) the "double arc" is not plainly obvious yet the authors make a point of discussing it at length; 2) the analysis of the simulations seems to lack an obvious direction. I would recommend acceptance if the issues below are addressed.

Primary items:

1) The "double arc" is not especially obvious in any of the panels of Fig. 3. It took me quite a while to fully recognize what structure the authors were talking about and to convince myself that it was not just a result of the contour intervals used. I'm not sure what the remedy is for this, but the double arc structure needs to be made clearer through either some enhancement of the figure, a schematic, or particularly lucid writing.

We added a figure (now Fig. 3; the old Fig. 3 is now Fig. 4) showing the DCC CFAD, with the double arc structure labeled on the graph.

2) I don't understand why the authors feel they can ignore graupel in SPV4. The model seems to include graupel to the same degree that it includes any physical species. It seems to be just as much a part of the precipitating ice category as snow.

Figs. 5-8 are now revised so that they include SPV4 output calculated using a single "precipitating ice" hydrometeor (the old SPV4 results), and SPV4 output calculated with the precipitating ice divided by diagnosed snow and graupel (dubbed SPG4 in the revised paper). The difference between the microphysical parameters used to represent precipitating ice in the radar simulator are much closer to those used for snow than for graupel, so it is reasonable to refer to precipitating ice as snow for simplicity. But as we are now including both variants of hydrometeor calculations in the paper, we can show that the inclusion of graupel in SPG4 results in only a modest change from the results of SPV4. There is still a notable difference between SPG4 and SPV5.

3) I don't think you have shown sufficient evidence to draw the conclusion you do on Line 285 (even if we all hope that this conclusion is true). Figure 6-9 show only that SPV5 behaves more logically. We do not know how the real world binned variables (reflectivity, SWC, etc) depend on W_{max}. And, I'm not sure I agree that the SPV5 CFAD is more like the CloudSat CFAD than the SPV4 CFAD; they share more characteristics with each other than they do with CloudSat. Perhaps you could add the difference between the CloudSat CFAD mean and those from both model runs to Fig. 5d. Or maybe you could compare the variance at each level.

Perhaps the word "significant" is too strong (as it is ambiguous outside of statistical definitions), but with the modifications to the results section, we do have sufficient evidence to make this conclusion. Bear in mind that Line 285 is the first line of a paragraph, and not meant to be taken out of context. Improving the reflectivity fields in DCCs will not occur as a result of one major change to the model, but as an incremental process through altering several different components of the model. Certainly SPV5 is closer to SPV4 than CloudSat, but it still shows improvement. Improving the microphysics alone won't make the simulation match the observations, but without improving the microphysics, the simulation will not match the observations.

I'm not sure how much useful information a rigorous comparison between the CloudSat and SP-CAM CFADs will provide, as it's pretty obvious where the deficiencies in the simulated CFADs lie. Of course we can include one if you think it is vital for the paper. Keep in mind simple methods for quantifying the differences between simulations and observations will not identify the missing double-arc reflectivity structure in the simulations – developing a method to do this might be useful in the future when models improve, but is probably overkill for now.

Other items:

Line 34: But Fu et al (1990) uses passive sensors. It should be made clear that the second two citations use models.

The latter two use models, but also observations. Lin et al. use passive sensors as well as TRMM PR, and Zhang et al. use passive radiance and TRMM PR. The point of the citations are to support the claim of the time lag, which is shown in both observations and (some) models.

Line 42: "There exist lidars" is awkward phrasing.

exist -> are

Line 57 to 63: These lines describe the most significant impact this paper will make several pages later.

Line 88: You might want to rephrase "temporal data domain".

temporal data domain -> time domain for the analysis

Line 107: Up to this point, you have not explained what scientific purpose you have in focusing on DCC. Is there a reason we expect Amazonian DCC to be especially microphysically variable?

Much of section 1 is devoted to explaining why we are studying DCCs, and why we chose the Amazon as the place of study. If you find the explanation insufficient, feel free to elaborate on what you think is missing. We don't have a specific a priori reason to expect enhanced microphysical variability in the Amazon above other convectively-active continental regions. We might expect the Amazon to show a range of microphysical characteristics because 1) the variety of convective organizations observed in the Amazon (single cell vs. coastal squall line vs. basin-wide MCC-like clusters), and 2) the variability in aerosol properties of the convective environment. The latter is an interesting possibility, and a possible future topic of investigation, as per RC2's suggestion.

Line 110: You may want to make it clearer that Fig. 2 does not use your DCC selection.

It does in the middle row, as the caption indicates. To help the reader in understanding section 3.1, we added the sentence "First, we will look at the frequency of all cloud types, and then subset the clouds into DCCs and anvils."

Line 122-123: These two sentences seem contradictory.

The wording is ambiguous. What we meant to say is that in the upper troposphere below 12.5 km, clouds are more frequent during night than day. Above 12.5 km, the opposite is true, suggesting that high clouds are less frequent during the day than night, but occur at higher altitudes. The text has been altered to clarify.

Figure 3a: What does "Quad" signify?

All four seasons: wet, dry, wet-to-dry, and dry-to-wet. This has been added to the figure caption.

Line 150: How do you know that neglecting to separate the data is the reason the double arc has not shown up before? It seems like you could show your selected-CFAD and an all data-CFAD.

Here is the all-data (i.e. all-sky) CFAD (note the color scale is adjusted to account for the absolute frequency difference):

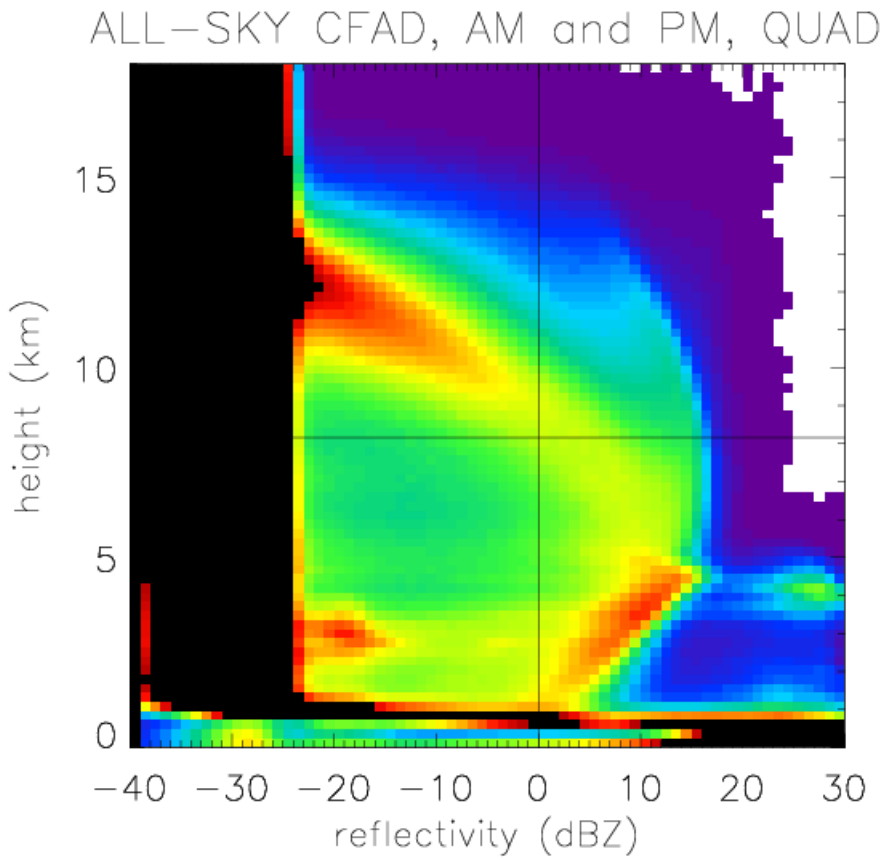

In the CFAD, above 8 km, the low reflectivity arc is much more prominent than the high reflectivity arc. Note than in this particular CFAD, the high reflectivity arc manifests as distinct from the low reflectivity arc, even though it isn't as obviously apparent as the other arc. This is not true for all CFADs shown for convectively-active areas in past research (like those in the cited publications). Clearly, limiting the data to DCC-only makes the two arcs much more distinct, and conversely including all data in a CFAD greatly reduces the contrast. But limiting the data to DCCs only appears to not be the sole factor – other things like the size of the frequency bins, number of observations, etc. are also important. In addition, it may be that the double-arc structure itself is more prominent in some regions than others. We haven't systemically investigated this yet, but we know from our past work that the double-arc structure appears in the tropical oceans (shown by Dodson et al. (2013)) and the contiguous United States (unpublished).

*So the line in question is mostly justified. We modified the statement to read "…**largely** because the DCCs are not cleanly separated from other cloud types…", because the separation of the data by cloud type is not the sole reason the double-arc structure is prominent in our results.*

Line 167: I'm not sure what the author is implying through the end of this paragraph.

The comparison of different metrics of convective activity is the topic of a paper of ours currently in preparation. We show that different metrics of convective activity can give different, or even contradictory, answers on analysis methods that depend on convective metrics (in our case the monthly variability in the Amazonian radiative diurnal cycle). It's inspired by the results of Liu et al. (2007). As our paper discussing this is not yet submitted, it is still premature to go into the details in the current paper under review. So to clarify our intentions, we added the sentence "Liu et al. suggest that this metric may be more useful for characterizing convective intensity than cloud top height, a traditional convective metric."

Figure 3j: The standard deviation of what? Or is it the difference of the standard deviations?

The standard deviation of the monthly mean day-night contrasts. As this quantity is not relevant for this paper, the standard deviation line has been removed.

Line 192: Why not show Wet-Dry differences in an additional column (like PM-AM differences are shown in an additional row)? Well, OK, the authors answer this question by the end of the paragraph by punting on seasonal differences. But if they want to do this (which they can), they should probably change the title of section 3.3 to just "Day versus night variability".

We address the wet-dry season contrast the best we can with the available data. Just because we are forced to punt on the dry season double arc doesn't mean that there is no useful information presented about the wet-dry season contrast. For example, we show that the mean reflectivity profile varies about four times as much in the day-night contrast as wet-dry. To our knowledge, this has not yet been shown by others with CloudSat data.

Line 220: How was the CRM sampled? Did you sample individual CRM grid columns in a way similar to CloudSat's sampling (i.e. approximately north-south at 1:30am/pm)?

We sample at 0200 and 1400 LST, which are the model output times closest to the CloudSat overpass times. This is now described in the text.

Line 226: I'm confused about what the authors mean throughout this paragraph. In SPV4, according to Wang et al (2011), SAM diagnoses all its microphysical species from predicted precipitating and non-precipitating water. Why do the authors feel they can "disregard diagnosed graupel" (and by that I assume they mean when running the radar simulator) and not, say, snow which seems to be diagnosed in the same manner as graupel? It seems like the authors should include graupel in their calculations and change their conclusion that SPV4 underestimates graupel. This would also make the paragraph beginning on Line 230 unnecessary.

See comment 2 above.

Line 238: Except SPV4 does "represent" graupel.

We mean it does not include graupel in the prognostic equations. This paragraph has been rewritten with regard to the inclusion of SPG4 results.

Figure 5: why use the dry season when the wet season produces the more significant "double-arc"?

As discussed in the text, the SP-CAM data we have are only available for the dry season. While ideally we would also have wet season data for comparison, it is very unlikely that wet season simulated convection has significantly more realistic reflectivity, let alone a double arc structure. Note despite the double-arc structure being

less defined in the dry season observed CFADs than wet season, the CFADs are otherwise much more similar to each other than the simulated CFADs.

The vertical velocities seem oddly low in magnitude. There is barely any weight to the PDFs above 1m/s (which would usually be considered "convective" in a CRM).

We've reproduced Fig. 5 using a modified definition of DCCs, where in addition to the criteria in the paper, we also excluded all vertical profiles where W_{max} is less than 1 m/s (here dubbed "ICCs" or (relatively) intense convective cores).

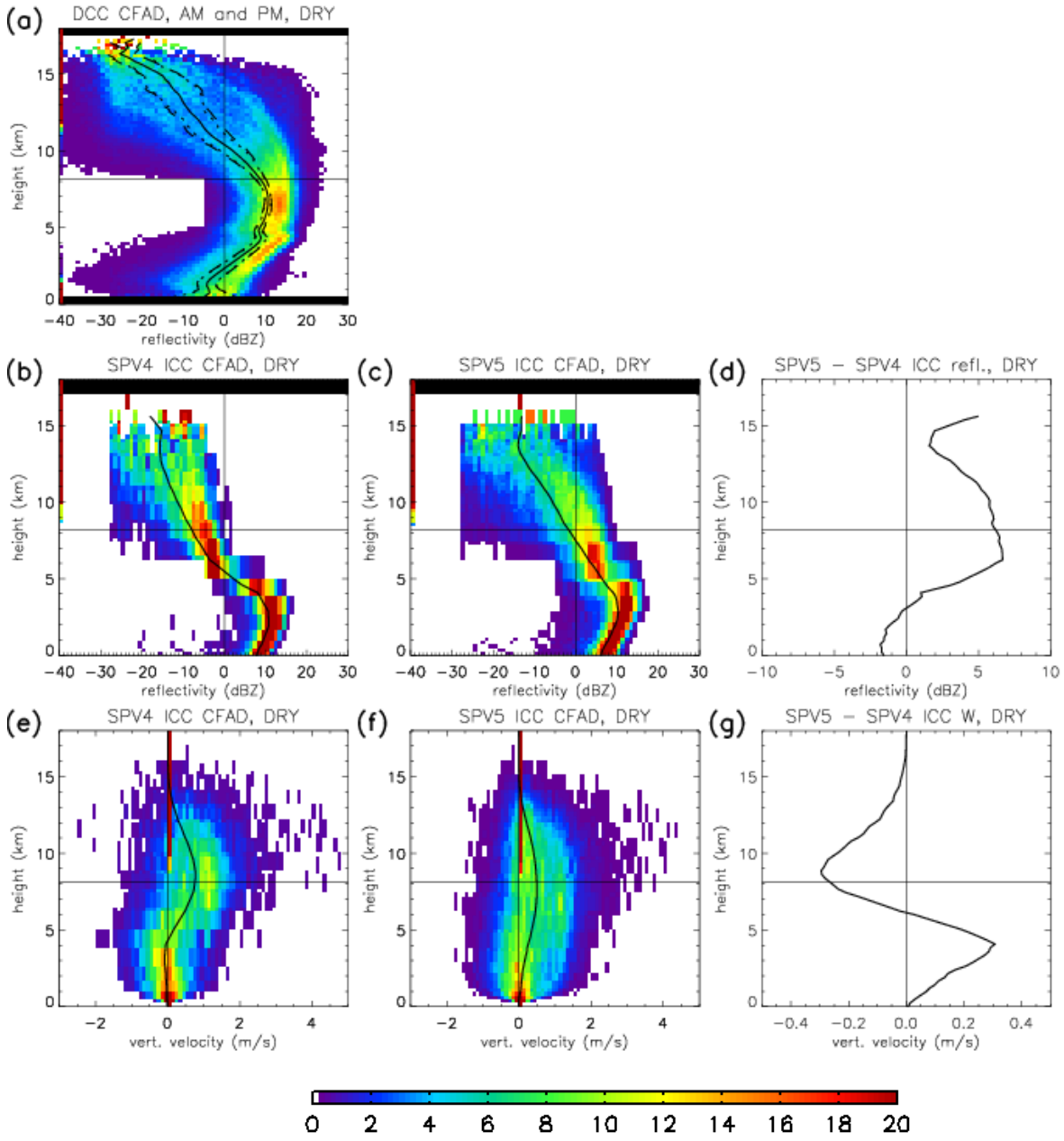

The reflectivity values in the mid- to upper troposphere are higher by ~5 dBZ for ICCs in SPV5, but there is no dramatic improvement in the reflectivity, nor is there a double-arc feature. The issue of low vertical velocity is now briefly discussed in the text of Section 4.

Figure 6: Realistically, I think one has to question the sampling at high Wmax when there are intermediate bins with zero samples. All the panels should probably be cutoff at ~3m/s. What are the different colored lines in panel (c)? Also, the label on the y-axis should probably be something like "fraction" rather than "count".

It is mentioned in the text that regression values are calculated from 0-2.5 m/s. The full data range are kept for completeness, but we added a vertical line as a reminder of where the cutoff for "useful" data is. The color lines represent night-only and day-only; this is now described in the caption. "Count" is changed to "fraction".

Line 264: This discussion of the "jump" needs to be clearer.

Some of the wording has been changed in this paragraph, specifically to highlight how a discontinuous jump would cause a double-arc structure, in other words a bimodal PDF in reflectivity in the upper troposphere.

Line 270: Or this logical thread about how the double arc structure might arise isn't correct. I don't have a different hypothesis to offer, but the reasoning seems appealing but unproven.

The other possibility is that the real PDF of W_{max} is bimodal, and the simulated PDFs are not. This is now discussed in the text. There are only three obvious logical possibilities for the discrepancy between the observed and simulated CFADs: the simulated distributions of reflectivity by W_{max} are unrealistic (i.e. Fig. 6a/6b/6c), the simulated PDFs of W_{max} are wrong (i.e. Fig. 6d), or both.

Anonymous Referee #2

In this study the authors use CloudSat data to analyze aspects of the microphysical properties of convective clouds over the Amazon. They show using the DBZ distributions vs. Height space (CFAD) several interesting features of these clouds. They show that when slicing per cloud type, clearer structural information appears that could be interpreted as contribution from specific hydrometeors type. Moreover, comparing the CFAD properties day vs. night and dry vs. wet season they could show shifts in cloud dynamics and microphysics. On the second part of the paper they check if numerical models can reproduce the CFAD properties. They compare two types of microphysical schemes and show that the two moment can produce results that are closer to the observations but still some of the main features are missing (such as the double arc shown in the observational part).

The first observational part of the paper reads well (less acronyms will make it even better) and it shows quite clearly the differences in the vertical hydrometeors distribution of convective cores, anvils and other clouds. The numerical modeling part is less clear and in my opinion does not stand on the same level of the first part. They start with a long discussion on why the models will fail before showing any results. Then they try to explain the dependency of the model results on updrafts comparing the two microphysical scheme.

Recommendations: (1) I would focus on the observational part making the paper clearer and shorter. The insights gained by the model experiments does not really explain the observations. The message that two moment microphysical scheme produces results that are more similar to the observations is interesting but then why not trying bin microphysics?

As per RC1, the observation section now has an additional figure that more clearly illustrates the double-arc feature in the observed CFADs. This seems to be the aspect of Section 3 that gave many people difficulty.

The purpose of the modeling results is not to explain the observations. Their purpose is to illustrate deficiencies in the simulated reflectivity, and suggest possible paths to reconcile simulated and observed reflectivity. This would

allow for more robust model/obs. intercomparisons using reflectivity as a metric. We have reorganized and rewritten portions of the modeling study in order to better integrate it with the overall narrative of the paper, specifically to convey this intent, and included a bit more analysis of the effects of microphysics on the simulated reflectivity (specifically the inclusion of diagnosed graupel).

Also, it is incorrect to discuss models in terms of failing (in a pass/fail sense), and we are certainly not attempting it in the (paragraph) long discussion at the start of Section 4. It is reasonable to discuss possible source of error in a model as a justification for the following analysis.

Finally, improving the microphysics is indeed a message of this paper, and using bin rather than bulk microphysics is a possible route for future models. However, the majority of CRMs today use bulk microphysics because bin microphysics are computationally expensive, and that extra computational power could be used for other purposes, e.g. increasing the spatial resolution. With Moore's law still in effect, the common use of bin microphysics will likely become feasible at some point in the foreseeable future, and so modeling experiments designed to test the benefits of bin over bulk microphysics will be valuable at that time.

(2) One additional analysis that could make the paper clearer and enhance the papers importance is to try to slice the data per aerosol loading. Such analysis should be doable using aerosol information near the observed clouds from the MODIS Aqua. Both the area and the topic of the paper are ideal for such study. Changes in the aerosol loading should directly affect the hydrometeors distribution and therefore should be reflected in the CFAD space. Specifically, in higher aerosol loadings I predict that the convective cores will be taller controlled by stronger updrafts. The onset of precipitation will be delayed but once rain starts it might be stronger. The effect on the ice particle distribution with height would be extremely interesting.

As we mentioned in the interactive comments, this is a very good idea, and something that is reasonably doable. However, we decided that this paper is not the best place for such an analysis, for several reasons.

1) In general, such an analysis is beyond the scope of this paper.

2) We're concerned that if we attempt to tack on an analysis of aerosol data to this paper, it would likely come off as a rushed, half-baked attempt to cram more into a paper that should have a complete narrative with just the observations and SP-CAM material. The effect of aerosols on convection is an important question, and one that deserves its own paper, and associated narrative.

3) Aerosols are complex. It probably would not be right to choose just a single variable for aerosols, such as total optical depth, but look at the effect of different aerosol properties (chemical species, size, vertical distribution) on convection. A rushed analysis would not allow sufficient time to investigate these different properties.

4) Unfortunately, the reviewer did not answer the question of whether CALIPSO data would be a useful alternative to MODIS data, or give particular motivation for using MODIS is particular. If we leave the aerosol analysis to a separate paper, we would have time to implement both datasets, and determine whether the results are dependent on the choice of dataset.

For these reasons, we will not include aerosols in this paper. However, we are strongly considering it as the topic for a future paper, and so we thank the reviewer for the suggestion.

Microphysical variability of Amazonian deep convective cores observed by CloudSat and simulated by a multi-scale modeling framework

J. Brant Dodson[1], Patrick C. ~~Taylor[1]~~Taylor[2], and Mark ~~Branson[2]~~Branson[3]

~~[1]NASA~~[1]Science Systems and Applications, Inc., Hampton, VA, USA
[2]Climate Science Branch, NASA Langley Research Center, ~~21 Langley Blvd., Mail Stop 420,~~ Hampton, VA, ~~23681-2199,~~ USA.
~~[2]Department~~[3]Department of Atmospheric Science, Colorado State University, Ft. Collins, CO ~~80523~~, USA

Correspondence to: J. Brant Dodson (jason.b.dodson@nasa.gov)

Abstract. Recently launched cloud-observing satellites provide information about the vertical structure of deep convection and its microphysical characteristics. In this study, CloudSat reflectivity data is stratified by cloud type, and the contoured frequency by altitude diagrams reveal a double-arc structure in deep convective cores (DCCs) above 8 km. This suggests two distinct hydrometeor modes (snow versus hail/graupel) controlling variability in reflectivity profiles. The day-night contrast in the double-arcs is about four times larger than the wet-dry season contrast. Using QuickBeam, the vertical reflectivity structure of DCCs is analyzed in two versions of the Superparameterized Community Atmospheric Model (SP-CAM) with single-moment (no graupel) and double-moment (with graupel) microphysics. Double-moment microphysics shows better agreement with observed reflectivity profiles; however, neither model variant captures the double-arc structure. Ultimately, the results show that simulating realistic DCC vertical structure and its variability requires accurate representation of ice microphysics, in particular the hail/graupel modes, though this alone is insufficient.

1 Introduction

As a driver of the hydrological cycle, the frequency and intensity of atmospheric deep convection influences spatial and temporal characteristics of precipitation. Our ability to simulate convective behavior on short (diurnal) and long (climate change) timescales significantly modifies projected changes in the spatiotemporal distribution of precipitation (including floods and drought), radiation, and other climate system elements (Arakawa, 1975). Simulating convection relies on our understanding of the physics controlling and modulating its behavior, including cloud microphysics, cloud scale dynamics (updraft/downdrafts), entrainment and other large-scale atmospheric interactions, cloud-surface interactions, and cloud-radiation interactions (Randall et al., 2003; Arakawa, 2004).

Atmospheric convection exhibits variability on multiple time scales, including diurnal and seasonal. The convective diurnal cycle (CDC), a well-documented and important mode of variability, is particularly pronounced over land (Yang and Slingo 2001, Nesbitt and Zipser 2003, Tian et al. 2004, Kikuchi and Wang, 2008; Yamamoto et al., 2008). The CDC is characterized by a rapid insolation-driven transition from shallow to deep convection in the early afternoon, followed by either a slow decay through the evening and early morning, or transition into mesoscale convective systems (MCSs), persisting into the next morning (Machado et al., 1998, Nesbitt and Zipser 2003). Geostationary satellite observations, in particular, have provided a global view of the spatial complexity of the CDC (Yang and Slingo, 2001). However, most satellite data sets only observe convective cloud top properties using passively-sensed visible and infrared radiances and cannot sense the cloud interior. With passive sensors, it is difficult to clearly distinguish between deep convective cores (DCCs) and related anvils, the latter having a diurnal cycle offset from DCCs by approximately three hours (e.g. Fu et al. 1990; Lin et al., 2000; Zhang et al., 2008).

A small number of satellites, such as CloudSat (Stephens et al., 2008), carry radars that penetrate cloud tops, sensing the interior of deep convection. Spaceborne radars allow the examination of deep convection invisible to most satellites, especially internal

structure and microphysics. CloudSat carries a W-band radar which is specifically attuned to observe smaller cloud liquid and ice hydrometeors. Other satellites, such as Tropical Rainfall Measuring Mission (TRMM) (Kummerow et al.; 1998) and the Global Precipitation Measurement (GPM) mission (Hou et al., 2014) are attuned to larger precipitation-sized hydrometeors. A sizable body of literature describes observations of tropical convection using these satellites (e.g. Petersen and Rutledge, 2001; Schumacher et al., 2004; Nesbitt and Zipser, 2003; Zipser and Nesbitt, 2007; Liu and Zipser, 2015; Liu and Liu, 2016). In addition to radars, there exist lidars such as that carried by Cloud-Aerosol Lidar and Infrared Pathfinder Satellite Observation (CALIPSO) (Winker et al., 2009), which has been used to examine the properties of convection and anvils (e.g., Sassen et al., 2009; Riihimaki and McFarlane, 2010; Del Genio et al. 2012).

Spaceborne cloud radars, precipitation radars, and lidars offer complementary views of tropical convection. Cloud radars sample the higher altitudes and anvils of DCCs, as well as associated stratiform clouds, but are ineffective at lower altitudes where precipitation-sized hydrometeors attenuate the radar beam. Precipitation radars examine the lower- and mid-level structure of DCCs, but cannot see cloud tops and anvils. Lidars are sensitive to the tops of thick clouds and can measure their altitude with high precision; however, they are unable to penetrate the tops of DCCs and most anvils. In this study, we will focus on the high-level features of DCCs and anvils, where CloudSat is most useful.

CloudSat's polar orbit, crossing the equator during early afternoon and early morning, provides two views of the CDC, near the beginning and end of the mean precipitation diurnal cycle over land. This ability has not been well-exploited in the literature. Liu et al. (2008) represents one of the few analyses on observed day-night differences using CloudSat. They surveyed day-night contrasts between reflectivity profiles over both tropical land and ocean, finding that high reflectivity clouds occur more frequently at night than during the day at all altitudes except at cloud tops (13 km). The authors interpret this difference as a consequence of the CDC, in which the peak in deep convective frequency occurs after the 1330 LST CloudSat overpass time, while there are still frequent lingering MCSs during the 0130 LST overpass. However, previous efforts muddle the physical interpretation by mixing the frequency of both shallow and deep convection, the vertical convective reflectivity profile, and the properties of other cloud types. Resolving these issues, we examine the day-night contrast in the reflectivity profile of mature deep convection after stratifying by cloud-type. This methodology allows the separation of convective frequency from the individual reflectivity profile signatures of different cloud-types, including those generated at different times in the convective life cycle, creating a clearer view of the day-night contrast.

The Amazon basin is an ideal location for studies of the CDC for multiple reasons. First, the Amazon has a well-defined, high-amplitude continental CDC, peaking regularly in the mid-afternoon (Yang and Slingo, 2001). Amazonia has a prominent recurring propagating coastal squall line, and various secondary local effects related to orography and the Amazon river (Janowiak et al., 2005; Burleyson et al., 2016). However, aside from the aforementioned squall line, it lacks the major diurnally propagating signals observed in other continental convective regions (e.g., the central United States and southern China) (Wallace et al., 1975; Dai et al., 1999; Zhou et al., 2008) that make generalizing regional CDC studies difficult. Second, Amazonia has a well-defined wet and dry season, allowing a seasonal examination of the CDC including distinct meteorological forcing for convection: locally-forced (common in the dry season) versus non-locally forced (common in the wet season). Finally, the Amazonian CDC alters the top-of-atmosphere radiative diurnal cycle (Taylor 2014a,b, Dodson and Taylor 2016), representing an influence on regional and global climate that meteorological reanalyses and climate models struggle to simulate (Yang and Slingo, 2001; Itterly and Taylor, 2014; Itterly et al. 2016).

This paper documents and describes a detailed view of the diurnal variability of the convective vertical structure observed by CloudSat. One of the key methods to accomplish this is to separate the variability in convective frequency from the variability in radar reflectivity. This new perspective not only clarifies previous findings, but also reveals a unique, previously unreported

double-arc structure in the average radar reflectivity profile of deep convection. This new finding relates to the ice microphysical structure relevant to convective dynamic and thermodynamic properties, including precipitation rate, downdraft and cold pool strength (affected by evaporation and sublimation of hydrometeors), latent heating vertical profile (and associated warming and drying of the convective environment), and detrained water mass (McCumber et al., 1991, Grabowski et al., 1999, Gilmore et al., 2004, Li et al., 2005). Based on our results, the simulation of deep convective characteristics, and the comparison between simulation and observations, benefits from a detailed representation of ice microphysics.

2 Data and Methodology

Cloud observations are taken from CloudSat, a cloud-observing member of the A-Train (Stephens et al., 2008), orbiting at 705 km altitude, 98° inclination, and equatorial crossing time of 1:30am/pm local time. The primary instrument is the Cloud Profiling Radar (CPR), a 94 GHz radar with a 1.1 km wide effective footprint and 480 m vertical resolution, oversampled to create a 240 m effective vertical resolution. CloudSat operated as designed from June 2006 to March 2011, until suffering a battery malfunction. This time period serves as the temporal data domain.

For cloud-type stratification, the CPR Cloud Mask and Radar Reflectivity fields from the 2B-GEOPROF product (Mace 2007) are used. The cloud-type stratification identifies 4 cloud types, DCCs, anvils (AVN), clouds attached contiguously with DCCs (CLD-D), and other clouds (CLD). DCCs are identified using a CPR-based methodology on a profile-by-profile basis (i.e. with no consideration to neighboring columns) according to three criteria from Dodson et al. (2013):

(1) must be at least 10 km tall,

(2) must have a continuous vertical region of reflectivity of at least -5 dBZ between 3 km and 8 km altitude, and

(3) the maximum reflectivity value at any altitude in the middle troposphere (3 km to 8 km) must be at least 0 dBZ.

The lower altitude bound in criterion 2 is raised to 5 km when heavy precipitation is detected (indicated by low surface reflectivity), accounting for attenuation effects. The latter two criteria restrict the set of profiles with deep cloud layers to those which likely contain active, vigorous DCCs only. These criteria are guided by the cloud definitions used in creating the 2B-CLDCLASS product (Wang and Sassen, 2001). When the data are stratified by these criteria, CloudSat observed 187,457 vertical profiles of DCCs in the Amazon over the time domain, with just less than half (92,071, or 49%) occurring during the daytime overpass.

Figure 1 shows the spatial domain of the analysis region, centered on northern and central South America (25°S – 0°S, 70°W – 50°W). In addition, a CloudSat overpass through the domain displays the associated cloud presence, morphologies, and radar reflectivity for a single overpass (Fig. 1a-c), displaying the identified cloud types in the bottom panel (Fig. 1d). This particular overpass provides an example of the stratification method, displaying a variety of deep convective cloud systems and associated anvils, including narrow single-cell updrafts to the north, and wider multi-celled convection to the south. Note, only a subset of the profiles within deep convective cloud systems are ~~labeled~~labelled DCCs – this is deliberate to include only the profiles which likely contain active convective updrafts.

3 Results

3.1 Mean cloud properties

Untangling the influence of convective frequency on the deep convective vertical reflectivity structure benefits from an examination of the mean CloudSat-observed cloud properties (Fig. 2). First, we will look at the frequency of all cloud types, and then subset the clouds into DCCs and anvils. Clouds occur in a layer between 1.5 km and 12 km, with small maxima in cloud

occurrence frequency (COF) at 11.5 km and 2.5 km (Fig. 2a). The cloud top height (CTH) vertical profile (Fig. 2b) shows four regions of interest – a primary maximum at 13 km a secondary maximum at 1.2 km, a broad enhanced frequency region between 2.5 and 6 km, and a small maximum at 7.5 km. The cloud base heights (CBHs, Fig. 2c) show a large primary maximum at 1.2 km, a broad secondary maximum centered at 11 km, and a small local maximum at 5 km. These features are consistent with the identified tri-modal vertical cloud structure in convectively-active tropical regions (Johnson et al., 1999; Khairoutdinov et al., 2009), with shallow convective clouds, cumulus congestus, and DCCs with associated anvils comprising the bulk of Amazonian clouds. The DCC-anvil and shallow cumulus modes are more prominent in the data than the cumulus congestus mode; this might be related to the greater variability of CTH for congestus than the other cloud types, which are constrained by the level of neutral buoyancy (for DCCs-anvils) and the atmospheric boundary layer top (for shallow cumulus).

Mean COF vertical profiles differ significantly between day and night, differences at most altitudes have p-values (two-tailed t-test) << 0.01. High (low) level clouds are enhanced during night (day), and the opposite suppressed. ~~However,~~ In addition, high altitude clouds (above 12.5 km~~, clouds~~) are more frequent during day than night~~, contrary to the rest of the upper troposphere~~. The CTH profiles (Fig. 2b) show a contribution to high level cloud frequency from a daytime CTH increase (i.e. taller DCCs, likely with overshooting tops), indicating that despite fewer daytime high clouds they are taller than those at night.

DCCs occur in 3% of CloudSat profiles over Amazonia (Fig. 2d), with mean CTH near 14 km (Fig. 2e). The tallest DCCs reach an altitude of 18 km, which penetrate the tropopause and likely contribute to stratosphere-troposphere interactions (Johnston and Solomon, 1979; Corti et al., 2008; Avery et al., 2017). DCCs are on average about 0.5 km taller during the day than night (also significant at p << 0.01). Anvil cloud frequency (Fig. 2g) peaks at 12 km, with anvil CTH (Fig. 2h) maximizing at 13.5 km (0.5 km lower than DCCs). Anvil bases occur in a broad layer between 5 km (by definition the lowest altitude) and 11 km, diminishing with height above (Fig. 2i). The 5 km lower limit of anvil bases (where 5 km is chosen as being near the freezing line) is evidentially an artificial limit imposed by the methodology, and there may be no clear distinction between anvil clouds and deeper free-tropospheric clouds in nature.

3.2 Deep convective reflectivity profiles

The frequency component of the data for various cloud types has been isolated and described, so now the vertical structure variability is open for examination. The mean vertical profile of reflectivity in DCCs over the Amazon, as well as the total variability, are presented as contoured frequency by altitude diagrams (CFADs), where the color shading represent the probability density function of reflectivity at each altitude (Fig. 3). Previous research (e.g. Bodas-Salcedo et al. 2008, Satoh et al. 2010, Nam and Quaas 2012) associates deep convection with a characteristic arc shape in the reflectivity CFAD, maximizing in the middle troposphere and decreasing at upper and lower altitudes. A similar shape is apparent in Fig. 3. Reflectivity is reduced near the surface from radar beam attenuation by raindrops (Sassen et al., 2007). The kink in the reflectivity profile at 5 km is a "dark band" marking enhanced beam attenuation from melting hydrometeors at the freezing level. Reflectivity in the higher cloud altitudes (above 7.5 km) decreases with height primarily through reduction in hydrometeor size – this is because, assuming Rayleigh scattering and ignoring phase changes, hydrometeor size dominates reflectivity (proportional to the sixth power of diameter) (Battan, 1973). Large hydrometeors fall out of the updraft more rapidly than small hydrometeors, leading to vertical size sorting.

The CFAD associated with the DCC vertical profile displays an interesting feature above 8 km. While the CFAD ~~arc~~ follows the ~~mean profile (Fig. 3)~~characteristic arc shape at ~~most~~lower altitudes, in the upper ~~cloud~~troposphere the CFAD splits into two arcs. The low-reflectivity arc decreases below 0 dBZ at 11 km, whereas the high-reflectivity arc remains above 0 dBZ at 14 km. The double-arc structure most likely indicates two different modes of hydrometeors: a low-reflectivity arc associated with ~~cloud ice and~~ snow and a high-reflectivity arc associated with graupel and hail. Cloud ice has typical reflectivity values below the minimum

detection threshold of CloudSat (-28 dBZ), and does not contribute as much to the CFAD as the other ice hydrometeor species.

This double-arc structure is not obvious (and thus unreported) in previous studies examining radar reflectivity profiles in deep convection (e.g. Bodas-Salcedo et al. 2008, Satoh et al. 2010, Nam and Quaas 2012) largely because the DCCs are not cleanly separated from other cloud types, leading to a blurred reflectivity structure.

How do we know that the double arcs are associated with different hydrometeor species? Figure ~~4~~5 shows the reflectivity CFADs for anvil clouds. Instead of a double-arc reflectivity structure above 8 km, anvils have a single arc with reflectivity well below 0 ~~dbZ~~dBZ above 10 km. The CFAD closely resembles the ones constructed by Yuan et al. (2011), specifically for thick anvils, where reflectivity values of 0 dBZ are frequent at altitudes of 8-10 km, and decreases rapidly with height. However, Yuan et al. show the reflectivity maximum extending 1-2 km higher in altitude than Fig. ~~4~~5 does.

This single reflectivity arc corresponds with the low reflectivity (i.e. snow) arc observed in DCCs. This result is consistent with the hydrometeors in anvils consisting of the snow and cloud ice detrained from DCCs (modified by cloud processes as the anvils age), while dense ice hydrometeors either fail to be detrained into the anvil or quickly sediment from the anvil base immediately adjacent to the DCC. This corresponds with in situ measurements of anvil hydrometeors from West African convection (Bouniol et al. 2010). Note that some graupel particles are likely detrained into the anvils produced by DCCs with strong updrafts (Cetrone and Houze, 2009). However, these particles are not large and/or numerous enough to create the double-arc structure in the anvil reflectivity CFADs.

The presence of two distinct groups of hydrometeors in the upper cloud indicates a fundamental mode of variability in the DCC reflectivity profile. Higher (lower) reflectivity in the upper cloud indicate a larger (smaller) ratio of hail/graupel particles to snow. Dense, large, reflective particles generated in DCCs with higher vertical velocities are lofted higher into the upper cloud (Liu et al., 2007), linking the upper cloud reflectivity to updraft velocity. This relationship can be used as a proxy metric of convective intensity, and compared with other convective properties (e.g., frequency, top height, precipitation, radiative effects, etc). Liu et al. suggest that this metric may be more useful for characterizing convective intensity than cloud top height, a traditional convective metric.

3.3 Day Versus Night and Wet versus Dry Season Variability

The DCC reflectivity profiles, in particular the CFAD double-arc structure, show significant day-night and wet-dry season variability. The day-night contrast results show the upper cloud reflectivity is larger during day than night, by up to 4.5 dBZ at 12.5 km (Fig. ~~3j~~4j-l, solid line), which is caused by a more prominent high-reflectivity arc during the day than night. This feature also supports the conclusion that daytime updraft velocities are higher than nighttime velocities. This is consistent with the continental CDC, as described previously. Nighttime convection (midway between the afternoon peak and morning lull) is likely to be weakening and/or transitioning to MCSs (Machado et al., 1998), and exist in an environment partially contaminated by earlier convection and not being rejuvenated by insolation (Chaboureau et al., 2004).

These results clarify the day-night contrast presented by Liu et al. (2008). In CloudSat observations, DCCs are more frequent during nighttime than daytime. However, the DCCs occurring during the daytime overpass have larger updraft velocities than those at night. The positive day-night reflectivity difference in the upper cloud extends well below 12 km (the altitude indicated by Liu et al. (2008)), and represents a day-night contrast in the microphysical properties of the ice phase in DCCs. In summary, DCCs observed during the daytime overpass are less frequent, but taller, with larger vertical velocities, and more ice hydrometeors in the hail/graupel phases, than the DCCs observed at night.

The double-arc reflectivity structure in the upper troposphere exhibits seasonal differences. Amazonian convection exhibits strong seasonal variations in the frequency and other properties because of changes in forcing mechanisms (Fu et al., 1999; Marengo et

al., 2001; Raia and Cavalcanti, 2008), also connected with variability in day-night contrasts. Figure ~~3~~4 shows the day-night contrast in DCC reflectivity profiles during the wet and dry seasons. Season-specific results show the same qualitative pattern as the annual results – higher reflectivity during day (night) than night in the upper (lower) cloud. The amplitude of the difference is similar in both seasons, but the altitudes of enhanced daytime reflectivity is limited to above 10 km in the dry season. Overall, the day-night radar reflectivity contrast is four to five times larger than the wet-dry season contrast, underscoring day-night contrasts as a major mode of deep convective variability.

The CFADs show additional differences between wet and dry seasons. Wet season CFADs show a well-defined double arc reflectivity structure in the upper cloud, whereas the dry season CFADs do not, particularly at night. This result might be a consequence of the drier thermodynamical environment and aerosol characteristics of the dry season environment (including anthropogenic aerosol from biomass burning) (e.g. Andreae et al., 2004; Lin et al., 2006). However, it may also be a sampling artifact due to the smaller number of DCCs during the dry season (9,616) versus the wet season (78,034). To test the sample size influence, we implement a Monte Carlo-style random sampling methodology to reduce the wet season sample size to that of the dry season. Reducing the sample size of the wet season to that of the dry season obscures the double-arc reflectivity structure (not shown), so the influence of seasonality on the double-arc structure cannot clearly be attributed to seasonal changes in the convective environment.

4 Comparison with simulated cloud from a multi-scale modeling framework

These findings raise questions about ongoing modelling studies that use simulated radar reflectivity as a metric for convective activity. The observed CFADs depict complex structure and variability in convective reflectivity. Can models replicate this? To investigate the ability of models to simulate the observed DCC vertical structure and the influence of microphysics, we use the Superparameterized Community Atmospheric Model (SP-CAM) (Khairoutdinov et al., 2005). SP-CAM is a multi-scale modeling framework (MMF) replacing the convective parameterization (among other things) of the Community Atmospheric Model (CAM) with a cloud-resolving model (the System for Atmospheric Modeling, described by Khairoutdinov and Randall (2003)), coupled within each GCM grid point. This is a study of opportunity, using data made available from past work, and so the time domain is limited to an Amazonian dry season in the early 21st century. Only data from 0200 and 1400 LST are included in this analysis, which are closest to the CloudSat overpass times of 0130 and 1330 LST. We use two versions of SP-CAM, employing single moment (SPV4) and double moment (SPV5) microphysics. Hydrometeor mixing ratios for cloud ice, cloud water, rain, snow, and graupel (double moment-only) taken from the cloud-resolving model (CRM) component of SP-CAM are used to simulate the associated 94 GHz reflectivity profile using the QuickBeam radar simulator (Haynes et al., 2007). The formulation of SPV5, and the differences between SPV4 and SPV5, are documented by Wang et al. (2011). The only major differences between SPV4 and SPV5 of direct relevance to deep convection are the microphysical and radiative parameterizations; we attribute primary differences between SPV4 and SPV5 to microphysics.

A major difference between the SPV4 and SPV5 microphysics is the treatment of precipitating hydrometeors. SPV4 has diagnostic variables for snow and graupel. The SPV4 microphysics scheme predicts only non-precipitating and precipitating hydrometeors, which are partitioned into frozen and liquid by temperature. Snow and graupel are diagnosed from frozen precipitating water. However, snow and graupel as distinct hydrometeor species do not play a role in the prognostic microphysical equations in SPV4. In contrast, snow and graupel are prognosed hydrometeor types in SPV5, and are treated as a distinct species in the prognostic microphysical equations. So in addition to the reflectivity field calculated from precipitating ice in SPV4, we examine the influence of partitioning the precipitating ice into diagnosed snow graupel on the simulated radar reflectivity field. This new variant of SPV4 is hereby referred to as SPG4. Note that there are no differences between SPV4 and SPG4 other than the reflectivity fields simulated

by QuickBeam. This lets us distinguish between the effects of adding graupel to the hydrometeor species, and the effect of switching from single- to double-moment microphysics. Because the hydrometeor parameters in QuickBeam are similar for precipitating ice and snow, the main effect of the partitioning is the increased reflectivity from diagnosed graupel.

It is difficult to directly compare satellite-retrieved and model-simulated convective cloud ice (Waliser et al., 2009). Radar reflectivity serves as a substitute basis for comparison, where model reflectivity is computed with a radar simulator. However, ice phase microphysical properties of DCCs are a key component in determining the model-simulated reflectivity profile. This creates a challenge for interpreting simulated reflectivity, as it is difficult to detangle the influence that model microphysics has on the simulated reflectivity profile and its relationship with other properties of simulated convection (e.g. vertical updraft velocity). Observed reflectivity profiles are affected by multiple ice hydrometeor types, including both snow and graupel/hail. In order for models to realistically simulate DCC reflectivity profiles, and thus allow for robust statistical reflectivity model/observation intercomparison (in the vein of Liu et al. (2008)), the models must simulate both ice hydrometeors realistically (a function of the microphysics) and the relationships between the hydrometeors and other aspects of convection (e.g. vertical velocity). Therefore, it is difficult to strictly and simply attribute model-observational differences to specific aspects of the parameterizations. Nevertheless, it is still possible and useful to show the aggregate effects that the choice of microphysics have on the simulated reflectivity field, and so (at least partially) account for model-observation differences.

~~To investigate the ability of models to simulate the observed DCC vertical structure and the influence of microphysics, we use the Superparameterized Community Atmospheric Model (SP-CAM) (Khairoutdinov et al., 2005). SP-CAM is a multi-scale modeling framework (MMF) replacing the convective parameterization (among other things) of the Community Atmospheric Model (CAM) with a cloud-resolving model (the System for Atmospheric Modeling, described by Khairoutdinov and Randall (2003)), coupled within each GCM grid point. This is a study of opportunity, using data made available from past work, and so the time domain is limited to an Amazonian dry season in the early 21st century. We use two versions of SP-CAM, employing single-moment (SPV4) and double-moment (SPV5) microphysics. Hydrometeor mixing ratios for cloud ice, cloud water, rain, snow, and graupel (double moment-only) taken from the cloud-resolving model (CRM) component of SP-CAM are used to simulate the associated 94-GHz reflectivity profile using the QuickBeam radar simulator (Haynes et al., 2007). The formulation of SPV5, and the differences between SPV4 and SPV5, are documented by Wang et al. (2011). The only major differences between SPV4 and SPV5 of direct relevance to deep convection are the microphysical and radiative parameterizations; we attribute primary differences between SPV4 and SPV5 to microphysics.~~

~~It should be noted that SPV4 has a diagnostic variable for graupel. However, this variable does not play a role in the prognostic microphysical equations in SPV4 – only total precipitation, which is partitioned into liquid and frozen by temperature. In contrast, graupel is a prognosed hydrometeor type in SPV5, and is treated as a distinct species in the prognostic microphysical equations. We will discuss only the prognosed hydrometeor types in the following sections. The inclusion of diagnosed graupel in the computation of results causes only minor changes to the results at most, so we disregard diagnosed graupel.~~

~~With the available data, we cannot distinguish completely between the effects of adding graupel to the hydrometeor species, and the effect of switching from single- to double-moment microphysics. The purpose of this section is not to attribute improvements in SPV5 radar reflectivity to a particular aspect of the microphysics, but rather to examine more generally the effect of improving the microphysics scheme on the simulated radar reflectivity field, with the goal of allowing more robust model-observation intercomparisons in mind.~~

4.1 Simulated reflectivity and vertical velocity profiles

Figure ~~5~~6 displays the CFADs of Amazonian DCCs for SPV4 and SPV5. Both versions produce reflectivity values above 5 km more than 10 dBZ lower than observed. Specifically, the observed graupel/hail branch of the reflectivity arc is missing in both model versions. SPV4 is particularly unrealistic, as the microphysics scheme does not represent graupel. SPG4 diagnoses graupel, but their effect on the reflectivity profile is minor. There is an enhancement of reflectivity of 2 dBZ at 6 km, and a 1-2 dBZ reduction of reflectivity elsewhere in the profile. This is a result of switching from nonprecipitating ice to snow in QuickBeam, meaning that including diagnosed graupel enhances the reflectivity profile by no more than 4 dBZ. SPV5 microphysics ~~represents~~predicts graupel, and the upper ~~cloud reflectivity~~ troposphere reflectivity is larger than SPG4, showing additional improvement in the switch in microphysical schemes. But SPV5 has a lesser (but still noticeable) disagreement with observations. ~~Neither~~No model variant reproduces the observed double-arc structure, suggesting a fundamental deficiency in representing the ~~behavior~~behaviour of large ice hydrometeors in convective updrafts.

~~Surprisingly, the disagreement~~Figure 7 shows that the convective updraft velocities in both SPV4 and SPV5 never exceed 5 ms^{-1}, which is unrealistically low for deep convection in the Amazon (Giangrade et al., 2016). This is likely a major contributor to the low reflectivity in the simulated reflectivity above 10 km, and is likely related to the coarse resolution of the CRM (Petch et al., 2002; Bryan et al., 2003; Khairoutdinov et al., 2009). However, vertical velocity is not the sole contributor to the size of the simulated reflectivity. Surprisingly, the disagreement between SPV4 and SPV5 does not directly correspond with a proportionally large change in simulated updraft velocity profile ~~(Fig. 5e-g).~~ Despite upper cloud reflectivity being higher in SPV5 than SPV4, mean updraft velocity in the upper cloud decreases (and turns positive in the lower troposphere). In addition, SPV4 DCCs have net negative velocity below 3 km. This may not seem like an intuitive result initially, and closer to the properties of stratiform precipitation. However, it likely represents the thermal "bubble" nature of atmospheric convection (Scorer and Ludlam, 1953; Batchelor, 1954; Carpenter et al., 1998; Sherwood et al., 2013; Morrison, 2017). The DCC-identification method favors columns with high reflectivity in the mid- to upper troposphere. These columns usually contain strong updrafts at the same altitudes, which is the convective updraft thermal. In contrast, near the surface, the high-buoyancy air has already been evacuated into the thermal aloft, leaving neutral or negatively buoyant air in the lower troposphere. The selection process is not perfect, and Fig. ~~5e~~7a and ~~5f~~7b shows that strong downdrafts are occasionally included in the set of DCC profiles. Nevertheless, the net sinking motion below 3 km in SPV4 is consistent with deep convection.

4.2 Simulated reflectivity stratified by updraft velocity

The argument we present relies critically on the relationship between convective updraft velocity, the graupel phase of microphysics, and radar reflectivity. These are difficult to unweave in the observations, because of lack of direct vertical velocity observations, and the limitations of microphysical retrievals (particularly in scenes with heavy precipitation for W-band radars (Mace et al., 2007)). However, it is possible to separate them in the simulation by stratifying vertical reflectivity and hydrometeor profiles by updraft velocity. In Figs. ~~6 9~~8-11, the CRM-level vertical profiles associated with DCCs are conditionally sampled by the maximum positive vertical velocity (denoted hereafter as W_{max}) occurring in each profile. The probability density function (PDF) of W_{max} is also displayed~~.~~ – note that the low W_{max} in SPV4 and SPV5 are not confined to either daytime or nighttime. Fig. ~~6~~8 shows that for ~~both~~ SPV4 ~~and~~SPG4, SPV5, CTH increases as W_{max} increases (with regression slopes of 1.50, 1.66, and 1.35 km $(m\ s^{-1})^{-1}$, respectively, when calculated between 0 m s^{-1} and 2.~~4~~5 m s^{-1}). Furthermore, the echo top heights (ETH) of low reflectivity values in the upper cloud (e.g., -10 dBZ, indicated by dark green) increase with W_{max} at similar rates as CTH for ~~both~~ SPV4, SPG4 and SPV5 (1.29, 1.28, and 1.64 km $(m\ s^{-1})^{-1}$). However, the ETH of larger reflectivity values such as 0 dBZ (indicated by yellow) increases almost negligibly with W_{max} for SPV4 (0.00 km $(m\ s^{-1})^{-1}$), compared with SPG4 and SPV5 (0.68 and 1.79

km (m s-^{1})$^{-1}$). And even with diagnosed graupel included, the slope of 0 dBZ ETH in SPG4 is only a third that of SPV5. This result confirms that the lower reflectivity in SPV4 DCCs compared with SPV5 and observations is not caused *solely* by weaker updrafts, and the microphysics scheme plays a key role in upper tropospheric reflectivity.

~~Furthermore~~There are two obvious simple possible causes for the lack of a double-arc CFAD structure in SPV5. First, note that for SPV5, the 0 dBZ ETH increases ~~monotonically~~steadily as W_{max} increases, and there is no discontinuous "step function" jump in ETH. The ~~(~~hypothetical~~)~~ presence of a discontinuous jump in ETH ~~at large~~as W_{max} ~~value~~increases would cause a ~~jump~~double-arc structure in the simulated CFAD, similar to ~~the observed double-arc structure.~~observations. In other words, the PDF in reflectivity in the upper troposphere would be bimodal, with the low (high) reflectivity mode representing DCCs with low (high) W_{max}. Such a jump could arise, for example, if graupel forms at only large values of W_{max}, which would discontinuously boost DCC reflectivity at high W_{max}. ~~In this~~This could also occur if hail was included in the microphysics. In this hypothetical case, the low W_{max} in SPV5 would cause the lack of the double-arc structure, because convective updraft velocity would rarely be large enough to cross the ETH jump at large W_{max}. Only the low reflectivity mode, i.e. the snow arc, of the CFAD would manifest. However, in the real case, this discontinuous jump does not exist in SPV5~~, so the lack of~~. If the discontinuous jump in reflectivity exists in reality, but the CRM fails to replicate it, then a double-arc structure in SPV5 is not caused simply by weak updrafts in SPV5.

The second possibility for the discrepancy is that the real PDF for W_{max} is bimodal, while the simulated PDFs have only one peak. Observed DCCs in the Amazon occur in three main organizational structures: afternoon disorganized "pop-up" convection, coastal squall lines, and basin-wide organized convection similar to oceanic mesoscale convective complexes (Tang et al., 2016). In addition, the Amazon has a wide range of aerosol environments, which may influence several properties of convection including updraft velocities (Andreae et al., 2004; Lin et al., 2006; Tao et al., 2012). These combination of effects may create a bimodal (or multi-modal) PDF of real W_{max}. While SP-CAM can represent certain properties of organized convection, such as diurnal propagation (Kooperman et al., 2013), the CRM does not allow realistic organization of convection. This contributes to a unimodal PDF of W_{max} which may be unrealistic. Until recently, the state of observations did not enable a robust analysis to test these two possibilities; large samples of DCC vertical velocity are difficult to collect. However, recent observations from field campaigns such as the Green Ocean Amazon experiment (Martin et al., 2016, 2017) may be useful for testing.

4.3 Hydrometeor variability by updraft velocity

How do the ice hydrometeor species contribute to radar reflectivity? Figures ~~7~~9 and ~~8~~10 show the change in snow water content (SWC) and graupel water content (GWC) with W_{max}, respectively. ~~Both~~In the case of SPV4, precipitating ice is classified as SWC. SPV4, SPG4, and SPV5 have SWC increasing at all altitudes above 5 km as W_{max} increases (146, 99, and 166 mg (m s^{-1})$^{-1}$, respectively), though SPV5 increases somewhat more rapidly than ~~SPV4 between 0 and 1.5 m s^{-1} (161 versus 113 mg (m s^{-1})$^{-1}$, respectively).~~the others. Because both models show similar relationships between SWC and W_{max}, SWC alone cannot explain the reflectivity differences. The result shown by Fig. ~~8~~10 can be summarized in two key points. First, SPV5 produces graupel at all values of W_{max}; therefore, the difference in reflectivity CFADs between SPV5 and the observations cannot be explained by the assumption that SPV5 simply has convective updrafts too weak to produce graupel. Second, the sensitivity of GWC to W_{max} is slightly greater than that of SWC (183 versus 166 mg (m s^{-1})$^{-1}$, respectively). This relatively rapid increase of GWC with W_{max} in SPV5 is the best explanation for the rise of the 0 dBZ ETH in SPV5, which is missing in SPV4. The increase in graupel with W_{max} in SPG4 (55 mg (m s^{-1})$^{-1}$) is much lower than that of SPV5, contributing to the lower radar reflectivity in SPG4.

Is the error in radar reflectivity for SPV4 related to changes in the convective updraft dynamics? Figure ~~9~~11 shows vertical velocity profiles sorted by W_{max} for SPV4 and SPV5~~.~~ (note that vertical velocity in SPV4 and SPG4 are identical). The vertical structure

for both SPV4 and SPV5 relate to W_{max} in similar manners, with relatively strong ascent above 5 km to the CTH for most values of W_{max}, and neutral to weak downdrafts below 5 km. It does not appear that the differences in radar reflectivity between SPV4 and SPV5 are related to differences in the vertical velocity profile.

Improving the microphysical parameterization in CRMs, including both adding ice-phase hydrometeor species and shifting from single- to double-moment microphysics, results in ~~significant~~noticeable improvements to the radar reflectivity fields associated with deep convection. This is consistent with previous studies which found improvements in the representation of deep convection as a result of the switch to multi-moment microphysics (e.g., Swann, 1998; Morrison et al., 2009; Dawson et al., 2010; Van Weverberg et al., 2012; Igel et al., 2015). ~~However~~However, it is also clear that there are other reasons for the low reflectivity in the upper troposphere, such as the weak updrafts in both versions of the models (which should increase with improved model dynamics and resolution). In addition, it appears insufficient to capture observed variability in the DCC vertical structure, such as the double-arc reflectivity structure. Further improvements in microphysics will likely be necessary for CRMs to produce the full observed variability in the reflectivity field. ~~Until that time, care should be taken when using radar simulators to compare models with observations, especially when variability in the reflectivity field is being examined.~~

5 Summary and Discussion

We have presented an analysis of the DCC vertical structure in the Amazon observed by CloudSat. While the vertical reflectivity structure of convectively-active areas has been examined previously, the methodologies mixed together the vertical structure of deep convection, the frequency of deep convection, and the attributes of other cloud types. To clarify, we separate vertical profiles from DCCs and examine the variability in the vertical structure. The results reveal a distinctive double-arc structure in the CFAD related to the relative frequencies of snow and graupel/hail in the upper cloud, depicting variability in microphysics and updraft velocities. The graupel/hail branch of the double arc is more prominent during early afternoon than early morning, indicated by higher upper cloud reflectivity during day than night. This indicates stronger updrafts in mature DCCs during day than night. The day-night contrast in reflectivity structure is roughly four times larger than the contrast between the wet season and dry season, indicating that the day-night contrast is a prominent mode of DCC variability.

The results show the importance of separating data by cloud type before interpretation. This allows for a clearer process-based analysis of satellite observations, rather than a statistical view that mixes meteorological processes reducing their utility for aiding model improvement and process-level understanding. Future research should display caution when directly comparing the statistics of observed reflectivity and simulated reflectivity, and drawing conclusions about the accuracy of simulated convection from reflectivity statistics alone.

In addition, our results indicate that cloud resolving and related models, such as MMFs, are unable to capture the previously unreported double-arc structure, representing a weakness in the simulation of convection and is at least in part due to ice microphysics. The model-data comparisons suggest significant model deficiencies in the representation of radar reflectivity associated with convection remain, however more sophisticated model physics (e.g. switching from single moment to double moment microphysics, including more ice hydrometeor species) can significantly improve the representation. Until that time, care should be taken when using radar simulators to compare models with observations, especially when variability in the reflectivity field is being examined. These findings aid us in interpreting the relationship between radar reflectivity and convection, and particularly when comparing CloudSat observations with simulated reflectivity profiles in cloud resolving models.

Data availability. CloudSat data are available at the CloudSat Data Processing Center of Cooperative Institute of Research in the Atmosphere (http://www.cloudsat.cira.colostate.edu). SP-CAM data were provided upon request from the Center for Multi-Scale Modeling of Atmospheric Processes (http://www.cmmap.org).

Competing interests. The authors declare that they have no conflict of interest.

Acknowledgements. This work has been supported by NASA grant # NNH13ZDA001N-TERAQ, "The Science of Terra and Aqua"; by the National Science Foundation Science and Technology Center for Multi-Scale Modeling of Atmospheric Processes (CMMAP), managed by Colorado State University under cooperative agreement No. ATM-0425247; by Science Systems and Applications, Inc. under STARSSIII; and by the NASA Postdoctoral Program. The authors thank David A. Randall for providing assistance with using SP-CAM.

References

Andreae, M. O., D. Rosenfeld, P. Artaxo, A. A. Costa, G. P. Frank, K. M. Longo, and M. A. F. Silva-Dias: Smoking Rain Clouds over the Amazon, Science, 303, 5662, 1337-1342, DOI: 10.1126/science.1092779, 2004.

Arakawa, A.: Modelling clouds and cloud processes for use in climate models, The Physical Basis of Climate and Climate Modelling, GARP Publ. Ser., 16, World Meteorol. Organ., Geneva, Switzerland, 1975.

Arakawa, A.: The cumulus parameterization problem: Past, present, and future, J. Clim., 217, 2493–2525, 2004.

Avery, M. A., S. M. Davis, K. H. Rosenlof, H. Ye, and A. E. Dessler: Large anomalies in lower stratospheric water vapour and ice during the 2015–2016 El Niño, Nat. Geosci., 110, 405-410, doi: 10.1038/NGEO2961, 2017.

Batchelor, G. K.: Heat convection and buoyancy effects in fluids, Q.J.R. Meteorol. Soc., 80: 339–358, doi:10.1002/qj.49708034504, 1954.

Battan, L. J.: Radar Observations of the Atmosphere, University of Chicago Press, 324 pp, 1973.

Bryan, G. H., J. C. Wyngaard, and J. M. Fritsch: Resolution requirements for the simulation of deep moist convection, Mon. Wea. Rev., 131, 2394–2416, doi:10.1175/1520-0493(2003)131,2394:RRFTSO.2.0.CO;2, 2003.

Bodas-Salcedo, A., M. J. Webb, M. E. Brooks, M. A. Ringer, K. D. William, S. F. Milton, and D. R. Wilson: Evaluating cloud systems in the Met Office global forecast model using simulated CloudSat radar reflectivities, J. Geophys. Res., 113, D00A13, doi:10.1029/2007JD009620, 2008.

Bouniol, D., Delanoë, J., Duroure, C., Protat, A., Giraud, V. and Penide, G.: Microphysical characterisation of West African MCS anvils, Q.J.R. Meteorol. Soc., 136, 323–344, 2010.

Burleyson, C. D., Z. Feng, S. M. Hagos, J. Fast, L. A. T. Machado, and S. T. Martin: Spatial variability of the background diurnal cycle of deep convection around the GoAmazon2014/5 field campaign sites, J. Appl. Meteorol. Climatol., 55, 1579–1598, doi:10.1175/JAMC-D-15-0229.1, 2016.

Carpenter, R. L., K. K. Droegemeier, and A. M. Blyth: Entrainment and Detrainment in Numerically Simulated Cumulus Congestus Clouds. Part III: Parcel Analysis, J. Atmos. Sci., 55, 3440-3455, 1998.

Cetrone, J., and R. A. Houze, Jr.: Anvil clouds of tropical mesoscale convective systems in monsoon regions, Q. J. R. Meteorol. Soc., 135, 305–317, doi: 10.1002/qj.389, 2009.

Chaboureau, J.-P., F. Guichard, J.-L. Redelsperger, and J.-P. Lafore: The role of stability and moisture in the diurnal cycle of convection over land, Q. J. R. Meteorol. Soc., 130, 3105–3117, doi: 10.1256/qj.03.132, 2004.

Corti, T., and coauthors: Unprecedented evidence for deep convection hydrating the tropical stratosphere, Geophys. Res. Lett., 35, L10810, doi:10.1029/2008GL033641, 2008.

Dai, A., F. Giorgi, and K. E. Trenberth: Observed and model-simulated diurnal cycles of precipitation over the contiguous United States, J. of Geophys. Res., 104(D6), 6377-6402, 1999.

Dawson, D. T., M. Xue, J. A. Milbrandt, and M. K. Yau: Comparison of evaporation and cold pool development between single-moment and multimoment bulk microphysics schemes in idealized simulations of tornadic thunderstorms, Mon. Wea. Rev., 138, 1152–1171, doi:10.1175/2009MWR2956.1, 2010.

Del Genio, A. D., Y. Chen, D. Kim, and M.-S. Yao: The MJO transition from shallow to deep convection in CloudSat/CALIPSO data and GISS GCM simulations, J. Clim., 25, 3755–3770, 2012.

Dodson, J. B., D. A. Randall, and K. Suzuki: Comparison of observed and simulated tropical cumuliform clouds by CloudSat and NICAM, J. Geophys. Res. Atmos., 118, 1852–1867, doi:10.1002/jgrd.50121, 2013.

Dodson, J. B., and P. C. Taylor: Sensitivity of Amazonian TOA flux diurnal cycle composite monthly variability to choice of reanalysis, J. Geophys. Res. Atmos., 121, 4404–4428, doi:10.1002/2015JD024567, 2016.

Fu, R., D. Genio, D. Anthony, and W. B. Rossow: Behavior of deep convective clouds in the tropical Pacific deduced from ISCCP radiances, J. Clim., 3, 1129–1152, 1990.

Fu, R., B. Zhu, and R. E. Dickinson: How Do Atmosphere and Land Surface Influence Seasonal Changes of Convection in the Tropical Amazon?, J. Climate, 12, 1306-1321, 1999.

Gilmore, M. S., J. M. Straka, and E. K. Rasmussen: Precipitation and Evolution Sensitivity in Simulated Deep Convective Storms: Comparisons between Liquid-Only and Simple Ice and Liquid Phase Microphysics, Mon. Wea. Rev., 132, 1897-1916, 2004.

Grabowski, W., X. Wu, and M. Moncrieff: Cloud resolving modeling of tropical cloud systems during Phase III of GATE. Part III: Effects of cloud microphysics, J. Atmos. Sci., 56(14), 2384–2402, 1999.

Giangrande, S. E., T. Toto, M. P. Jensen, M. J. Bartholomew, Z. Feng, A. Protat, C. R. Williams, C. Schumacher, and L. Machado: Convective cloud vertical velocity and mass-flux characteristics from radar wind profiler observations during GoAmazon2014/5, J. Geophys. Res. Atmos., 121, 12,891–12,913, doi:10.1002/2016JD025303, 2016.

Haynes, J.M., R.T. Marchand, Z. Luo, A. Bodas-Salcedo, and G.L. Stephens: A multi-purpose radar simulation package: QuickBeam, Bull. Amer. Meteor. Soc., 88, 1723-1727, 2007.

Hou, A. Y., R. K. Kakar, S. Neeck, A. A. Azarbarzin, C. D. Kummerow, M. Kojima, R. Oki, K. Nakamura, and T. Iguchi: The global precipitation measurement (GPM) mission, Bull. Am. Meteorol. Soc., 95, 701–722, doi:10.1175/BAMS-D-13-00164.1, 2013.

Igel, A. L., M. R. Igel, and S. C. van den Heever: Make it a double? Sobering results from simulations using single-moment microphysics schemes, J. Atmos. Sci., 72, 910–925, doi:10.1175/JAS-D-14-0107.1, 2015.

Itterly, K. F., and P. C. Taylor: Evaluation of the tropical TOA flux diurnal cycle in MERRA and ERA-Interim retrospective analyses, J. Clim., 27(13), 4781–4796, 2014.

Itterly, K. F., P. C. Taylor, J. B. Dodson, and A. B. Tawfik: On the sensitivity of the diurnal cycle in the Amazon to convective intensity, J. Geophys. Res. Atmos., 121, 8186–8208, doi:10.1002/2016JD025039, 2016.

Janowiak, J. E., V. E. Kousky, and R. J. Joyce: Diurnal cycle of precipitation determined from the CMORPH high spatial and temporal resolution global precipitation analyses, J. Geophys. Res., 110, D23105, doi:10.1029/2005JD006156, 2005.

Johnson, R. H., T. M. Rickenbach, S. A. Rutledge, P. E. Ciesielski, and W. A. Schubert: Trimodal Characteristic of Tropical Convection, J. Clim., 12, 2397- 2418, 1999.

Johnston, H. S., and S. Solomon: Thunderstorms as possible micrometeorological sink for stratospheric water, J. Geophys. Res., 84(C6), 3155–3158, doi:10.1029/JC084iC06p03155, 1979.

Khairoutdinov, M. F., and D. A. Randall: Cloud resolving modeling of the ARM summer 1997 IOP: Model formulation, results, uncertainties, and sensitivities, J. Atmos. Sci., 60, 607–625, 2003.

Khairoutdinov, M., D. A. Randall, and C. DeMott: Simulations of the atmospheric general circulation using a cloud-resolving model as a superparameterization of physical processes, J. Atmos. Sci., 62, 2136–2154, 2005.

Khairoutdinov, M. F., S. K. Krueger, C.-H. Moeng, P. A. Bogenschutz, and D. A. Randall: Large-Eddy Simulation of Maritime Deep Tropical Convection, J. Adv. Model. Earth Syst., 1, 15, doi:10.3894/JAMES.2009.1.15, 2009.

Kikuchi, K., and B. Wang: Diurnal precipitation regimes in the global tropics, J. Clim., 21(11), 2680–2696, doi:10.1175/2007JCLI2051.1, 2008.

Kooperman, G. J., M. S. Pritchard, and R. C. J. Somerville: Robustness and sensitivities of central U.S. summer convection in the super-parameterized CAM: Multimodel intercomparison with a new regional EOF index, Geophys. Res. Lett., 40, 3287–3291, doi:10.1002/grl.50597, 2013.

Kummerow, C., W. Barnes, T. Kozu, J. Shiue, and J. Simpson: The Tropical Rainfall Measuring Mission (TRMM) sensor package, J. Atmos. Oceanic Technol., 15, 809–817, 1998.

Li, X., C.-H. Sui, K.-M. Lau, and W.-K. Tao: Tropical convective responses to microphysical and radiative processes: A 2D cloud-resolving modeling study, Meteorol. Atmos. Phys., 90, 245–259, 2005.

Lin, X., D. A. Randall, and L. D. Fowler: Diurnal variability of the hydrologic cycle and radiative fluxes: Comparisons between observations and a GCM, J. Clim., 13, 4159–4179, doi:10.1175/1520-0442(2000)013<4159:DVOTHC>2.0.CO;2, 2000.

Lin, J. C., T. Matsui, R. A. Pielke Sr., and C. Kummerow: Effects of biomass-burning-derived aerosols on precipitation and clouds in the Amazon Basin: a satellite-based empirical study, J. Geophys. Res., 111, D19204, doi:10.1029/2005JD006884, 2006.

Liu, C., and E. J. Zipser: The global distribution of largest, deepest, and most intense precipitation systems. Geophys. Res. Lett., 42, 3591–3595. doi: 10.1002/2015GL063776, 2015.

Liu, C., E. Zipser, and S. W. Nesbitt: Global distribution of tropical deep convection: Different perspectives from TRMM infrared and radar data, J. Clim., 20, 489–503, doi:10.1175/JCLI4023.1, 2007.

Liu, C., E. J. Zipser, G. G. Mace, and S. Benson: Implications of the differences between daytime and nighttime CloudSat observations over the tropics, J. Geophys. Res., 113, D00A04, doi:10.1029/2008JD009783, 2008.

Liu, N., and C. Liu: Global distribution of deep convection reaching tropopause in 1 year GPM observations, J. Geophys. Res. Atmos., 121, 3824–3842, doi:10.1002/2015JD024430, 2016.

Mace, G.: Level 2 GEOPROF product process description and interface control document algorithm version 5.3, 2007. [Available at http://www.cloudsat.cira.colostate.edu/ICD/2B-GEOPROF/2B-GEOPROF_PDICD_5.3.doc (last access 03/03/2017).]

Mace, G. G., R. Marchand, Q. Zhang, and G. Stephens: Global hydrometeor occurrence as observed by CloudSat: Initial observations from summer 2006, Geophys. Res. Lett., 34, L09808, doi:10.1029/2006GL029017, 2007.

Machado, L. A. T., W. B. Rossow, R. L. Guedes, and A. W. Walker: Life Cycle Variations of Mesoscale Convective Systems over the Americas, Mon. Wea. Rev., 126, 1630-1624, 1998.

Marengo, J. A., B. Liebmann, V. E. Kousky, N. P. Filizola, I. C. Wainer: Onset and End of the Rainy Season in the Brazilian Amazon Basin, J. Climate, 14, 833-852, 2001.

Martin, S. T., and coauthors: Introduction: Observations and Modeling of the Green Ocean Amazon (GoAmazon2014/5), Atmos. Chem. Phys., 16, 4785–4797, doi: 10.5194/acp-16-4785-2016, 2016.

Martin, S. T., and coauthors: The Green Ocean Amazon Experiment (GoAmazon2014/5) Observes Pollution Affecting Gases, Aerosols, Clouds, and Rainfall over the Rain Forest, Bull. Am. Meteorol. Soc., 98:5, 981-997, doi: 10.1175/BAMS-D-15-00221.1, 2017.

McCumber, M., W.-K. Tao, J. Simpson, R. Penc, and S.-T. Soong: Comparison of ice-phase microphysical parameterization schemes using numerical simulations of tropical convection, J. Appl. Meteorol., 30, 985–1004, 1991.

Morrison, H.: An Analytic Description of the Structure and Evolution of Growing Deep Cumulus Updrafts, J. Atmos. Sci., 74, 809-834, doi: 10.1175/JAS-D-16-0234.1, 2017.

Morrison, H., G. Thompson, and V. Tatarskii: Impact of cloud microphysics on the development of trailing stratiform precipitation in a simulated squall line: Comparison of one- and two-moment schemes, Mon. Wea. Rev., 137, 991–1007, doi:10.1175/2008MWR2556.1, 2009.

Nam, C., and J. Quaas: Evaluation of clouds and precipitation in the ECHAM5 general circulation model using CALIPSO and CloudSat satellite data, J. Clim., 25(14), 4975–4992, 2012.

Nesbitt, S. W., and E. J. Zipser: The diurnal cycle of rainfall and convective intensity according to three years of TRMM measurements, J. Climate, 16, 1456–1475, doi:10.1175/1520-0442-16.10.1456, 2003.

Petch, J. C., A. R. Brown, and M. E. B. Gray: The impact of horizontal resolution on the simulations of convective development over land, Q. J. R. Meteorol. Soc., 128, pp. 2031–2044, 2002.

Petersen, W. A., and S. A. Rutledge: Regional variability in tropical convection: Observations from TRMM, J. Clim., 14, 3566–3586, 2001.

Raia, A., and I. F. A. Cavalcanti: The Life Cycle of the South American Monsoon System, J. Climate, 21, 6227-6246, 2008.

Randall, D., M. Khairoutdinov, A. Arakawa, and W. Grabowski: Breaking the cloud parameterization deadlock, Bull. Am. Meteorol. Soc., 84(11), 1547, 2003.

Riihimaki, L. D., and S. A. McFarlane: Frequency and morphology of tropical tropopause layer cirrus from CALIPSO observations: Are isolated cirrus different from those connected to deep convection?, J. Geophys. Res., 115, D18201, doi:10.1029/2009JD013133, 2010.

Sassen, K., S. Matrosov, and J. Campbell: CloudSat spaceborne 94 GHz radar bright bands in the melting layer: An attenuation-driven upside-down lidar analog, Geophys. Res. Lett., 34, L16818, doi:10.1029/2007GL030291, 2007.

Sassen, K., Z. Wang, and D. Liu: Cirrus clouds and deep convection in the tropics: Insights from CALIPSO and CloudSat, J. Geophys. Res., 114, D00H06, doi:10.1029/2009JD011916, 2009.

Satoh, M., T. Inoue, and H. Miura: Evaluations of cloud properties of global and local cloud system resolving models using CALIPSO and CloudSat simulators, J. Geophys. Res., 115, D00H14, doi:10.1029/2009JD012247, 2010.

Schumacher, C., R. A. Houze Jr., and I. Kraucunas: The tropical dynamical response to latent heating estimates derived from the TRMM Precipitation Radar, J. Atmos. Sci., 61, 1341–1358, 2004.

Scorer, R. S. and Ludlam, F. H.: Bubble theory of penetrative convection, Q.J.R. Meteorol. Soc., 79, 94–103, doi:10.1002/qj.49707933908, 1953.

Sherwood, S. C., D. Hernández-Deckers, and M. Colin: Slippery Thermals and the Cumulus Entrainment Paradox; J. Atmos. Sci., 70, 2426-2442, 2013.

Stephens, G. L., and coauthors: CloudSat mission: Performance and early science after the first year of operation, J. Geophys. Res., 113, D00A18, doi:10.1029/2008JD009982, 2008.

Swann, H.: Sensitivity to the representation of precipitating ice in CRM simulations of deep convection, Atmos. Res., 47–48, 415–435, doi:10.1016/S0169-8095(98)00050-7, 1998.

Tang, S., and coauthors: Large-scale vertical velocity, diabatic heating and drying profiles associated with seasonal and diurnal variations of convective systems observed in the GoAmazon2014/5 experiment, Atmos. Chem. Phys., 16, 14249-14264, https://doi.org/10.5194/acp-16-14249-2016, 2016.

Tao, W.-K., J.-P. Chen, Z. Li, C. Wang, and C. Zhang: Impact of aerosols on convective clouds and precipitation, Rev. Geophys., 50, RG2001, doi:10.1029/2011RG000369, 2012.

Taylor, P. C.: Variability of monthly diurnal cycle composites of TOA radiative fluxes in the tropics, J. Atmos. Sci., 71, 754–776, doi:10.1175/JAS-D-13-0112.1, 2014a.

Taylor, P. C.: Variability of Regional TOA Flux Diurnal Cycle Composites at the Monthly Time Scale, J. Atmos. Sci., 71, 3484-3498, doi: 10.1175/JAS-D-13-0336.1, 2014b.

Tian, B., B. J. Soden, and X. Wu: Diurnal cycle of convection, clouds, and water vapor in the tropical upper troposphere: Satellites versus a general circulation model, J. Geophys. Res., 109, doi:10.1029/2003JD004117, 2004.

Van Weverberg, K., A. M. Vogelmann, H. Morrison, and J. A. Milbrandt: Sensitivity of idealized squall-line simulations to the level of complexity used in two-moment bulk microphysics schemes, Mon. Wea. Rev., 140, 1883–1907, doi:10.1175/MWR-D-11-00120.1, 2012.

Waliser, D., and coauthors: Cloud ice: A climate model challenge with signs and expectations of progress, J. Geophys. Res., 114, D00A21, doi:10.1029/2008JD010015, 2009.

Wallace, J. M.: Diurnal variations in precipitation and thunderstorm frequency over the conterminous United States, Mon. Weather Rev., 103, 406–419, 1975.

Wang, M., and coauthors: The multi-scale aerosol-climate model PNNL-MMF: model description and evaluation, Geosci. Model Dev., 4, 137–168, 2011.

Wang, Z., and K. Sassen: Cloud type and macrophysical property retrieval using multiple remote sensors, J. Appl. Meteorol., 40, 1665–1682, 2001.

Winker, D. M., M. A. Vaughan, A. Omar, Y. Hu, K. A. Powell, Z. Liu, W. H. Hunt, and S. A. Young: Overview of the CALIPSO Mission and CALIOP data processing algorithms, J. Atmos. Oceanic Technol., 26, 2310–2323, doi:10.1175/2009JTECHA1281.1, 2009.

Yamamoto, M. K., F. A. Furuzawa, A. Higuchi, and K. Nakamura: Comparison of diurnal variations of precipitation systems observed by TRMMPR, TMI, and VIRS, J. Clim., 21, 4011–4028, 2008.

Yang, G.-Y., and J. Slingo: The diurnal cycle in the tropics, Mon. Wea. Rev., 129, 784–801, doi:10.1175/1520-0493(2001)129,0784:TDCITT.2.0.CO;2, 2001.

Yuan, J., R. A. Houze Jr., and A. J. Heymsfield: Vertical structures of anvil clouds of tropical mesoscale convective systems observed by CloudSat, J. Atmos. Sci., 68, 1653–1674, doi:10.1175/2011JAS3687.1, 2011.

Zhang, Y., and coauthors: On the diurnal cycle of deep convection, high-level cloud, and upper troposphere water vapor in the Multiscale Modeling Framework, J. Geophys. Res., 113, doi: 10.1029/2008JD009905, 2008.

Zhou, T., R. Yu, H. Chen, A. Dai, and Y. Pan: Summer precipitation frequency, intensity, and diurnal cycle over China: A Comparison of Satellite Data with Rain Gauge Observations, J. Clim., 21(16), 3997–4010, 2008.

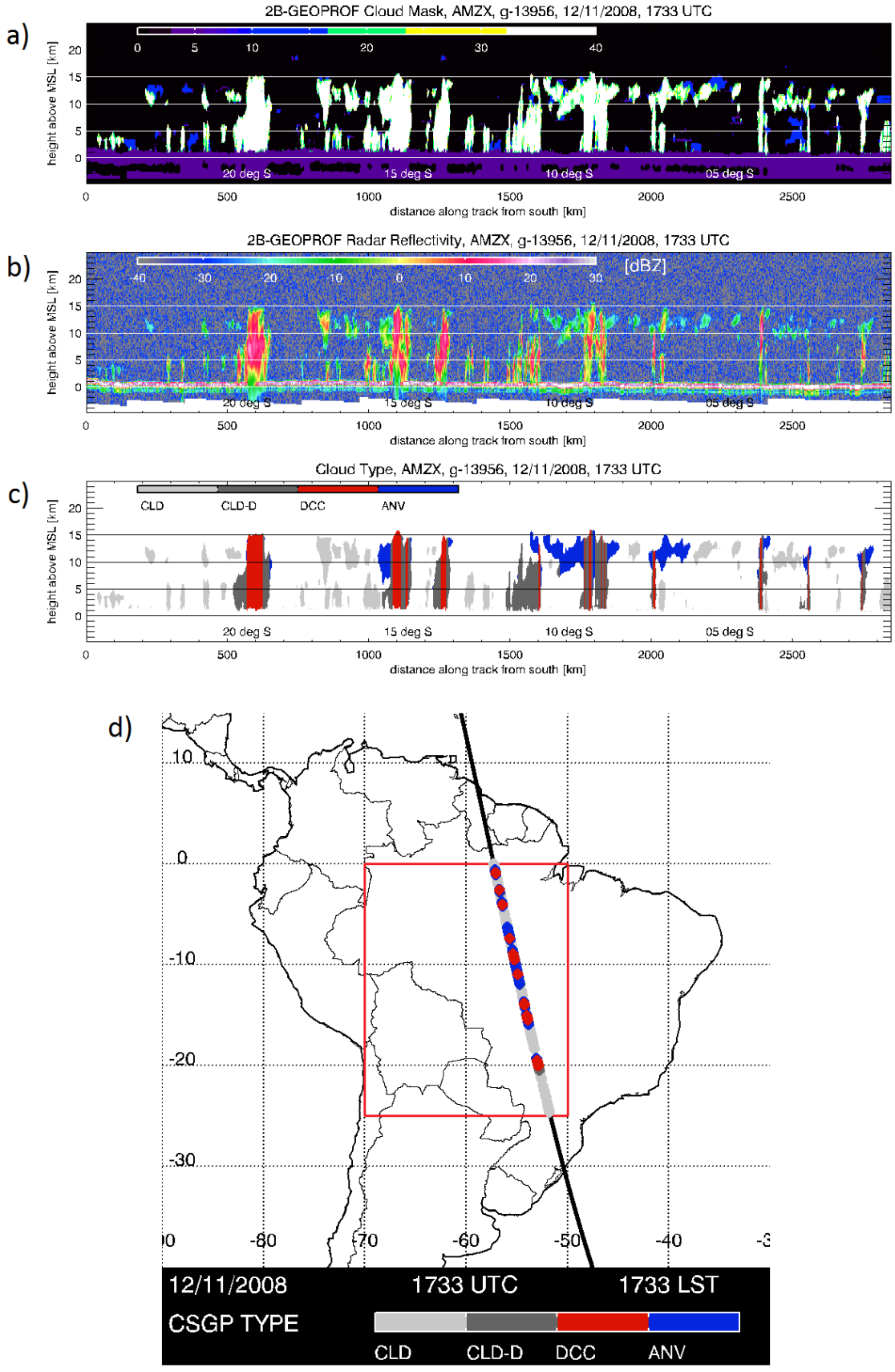

Figure 1. (a-c) Example of a CloudSat cross-sectional observation of afternoon convection on 11 December 2008 at approx. 1733 UTC (1333 LST). Left-to-right on the x-axis corresponds with south-to-north. (a) is the cloud mask product from 2B-GEOPROF, with colors representing the cloud mask value corresponding with certainty of cloud identification. (b) is radar reflectivity, and (c) is cloud type.

Red indicates DCCs, anvils are indicated with blue, dark gray indicates clouds attached contiguously with DCCs, and light gray indicates other clouds.

(d) Map of northern South America with the study region (25°S – 0°S, 70°W – 50°W) marked with the red box. The heavy black line crossing the study region indicates the path of the CloudSat swath shown in the top panel. The dominant cloud type observed by CloudSat along the path is indicated by colored dots.

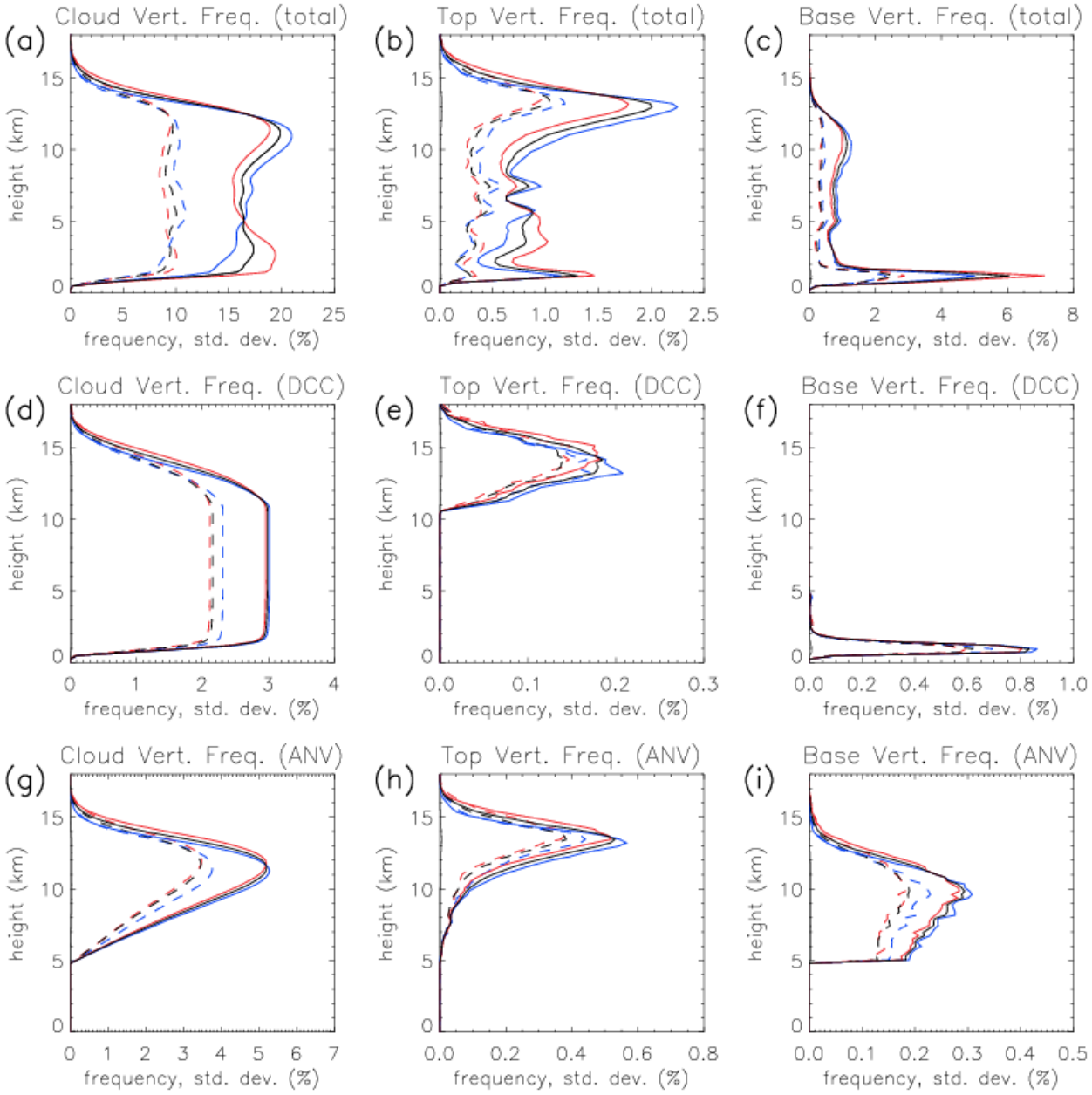

Figure 2. (Top) Vertical profiles of (a) cloud occurrence frequency (COF), (b) cloud top height (CTH) frequency (center), and (c) cloud base height (CBH) frequency. Black lines are for day/night, and red (blue) is for day-only (night-only). Solid (dashed) line is the mean (standard deviation)

(Middle) Same as top, but for (d) DCC-only COF, (e) CTH, and (f) CBH.

(Bottom) Same as top, but for (g) anvil-only COF, (h) CTH, and (i) CBH.

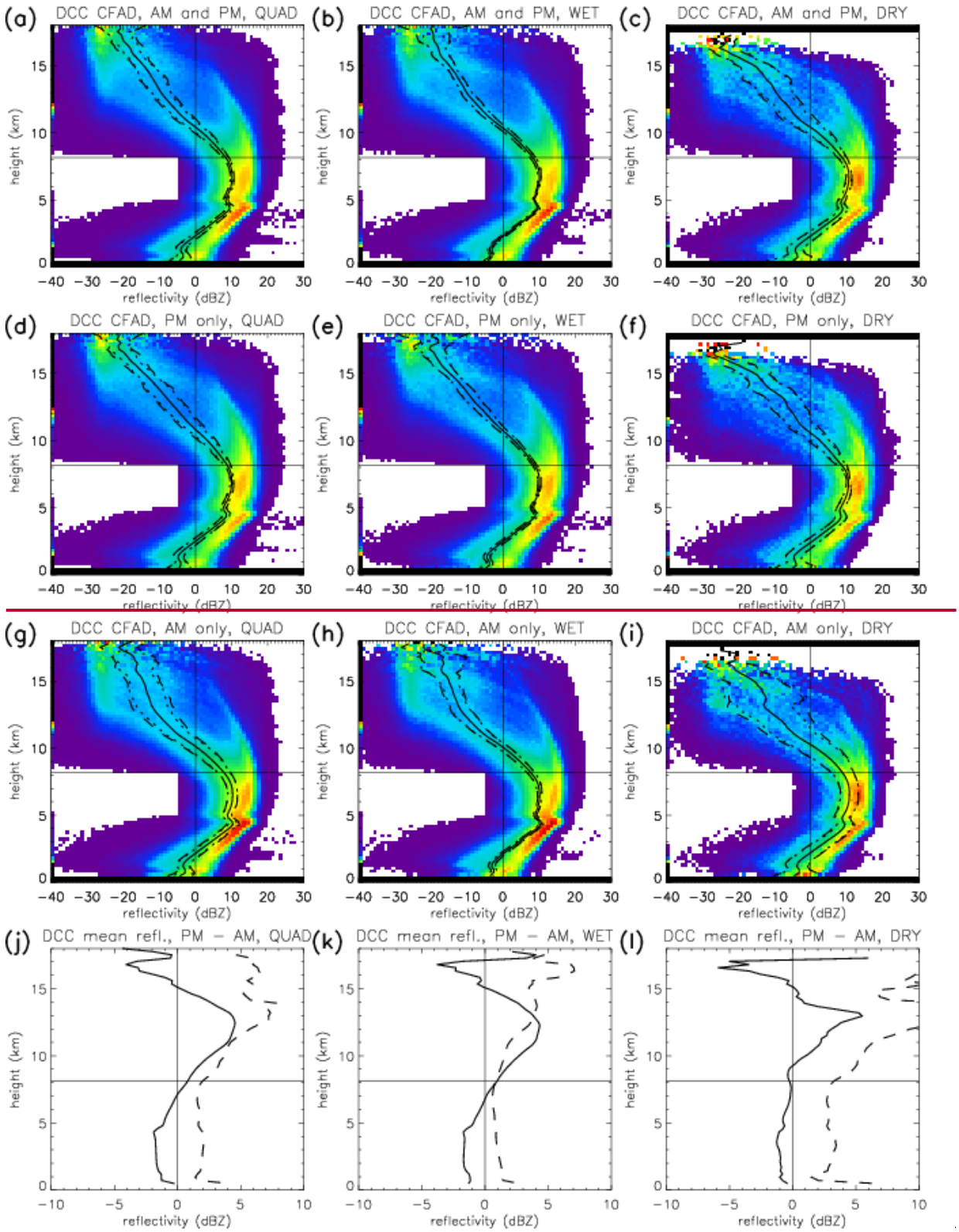
(a) DCC CFAD, AM and PM, QUAD
(b) DCC CFAD, AM and PM, WET
(c) DCC CFAD, AM and PM, DRY
(d) DCC CFAD, PM only, QUAD
(e) DCC CFAD, PM only, WET
(f) DCC CFAD, PM only, DRY
(g) DCC CFAD, AM only, QUAD
(h) DCC CFAD, AM only, WET
(i) DCC CFAD, AM only, DRY
(j) DCC mean refl., PM − AM, QUAD
(k) DCC mean refl., PM − AM, WET
(l) DCC mean refl., PM − AM, DRY
height (km)
reflectivity (dBZ)

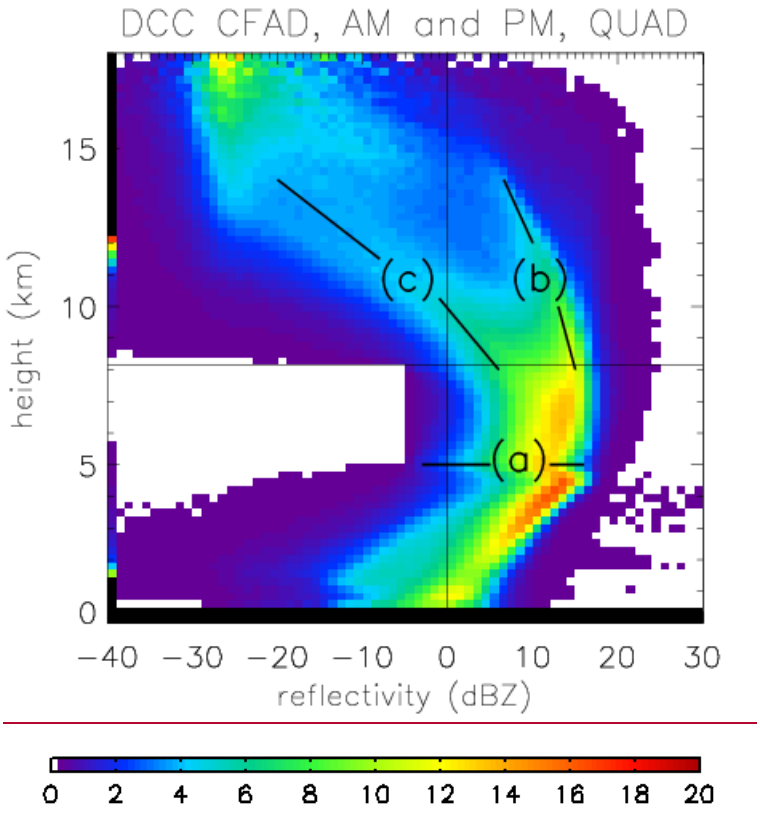

Figure 3. ~~**(a i)**~~ **The Contoured Frequency by Altitude Diagrams (CFADs) of reflectivity for DCCs in Amazonia. The colors** ~~**in each graph**~~ **represent the probability density function (PDF, as percentage) of radar reflectivity at each 240 m-tall layer observed by CloudSat. The vertical (horizontal) black line indicates 0 dBZ (8 km). Three distinct features of the CFAD, discussed in the text, are labelled on the figure. (a) indicates the dark band, with the horizontal line segments showing the mean altitude. (b) and (c) mark the locations of the high and low reflectivity arcs, respectively. The diagonal line segments show the orientation of each arc, and the rough values of the PDF modes.**

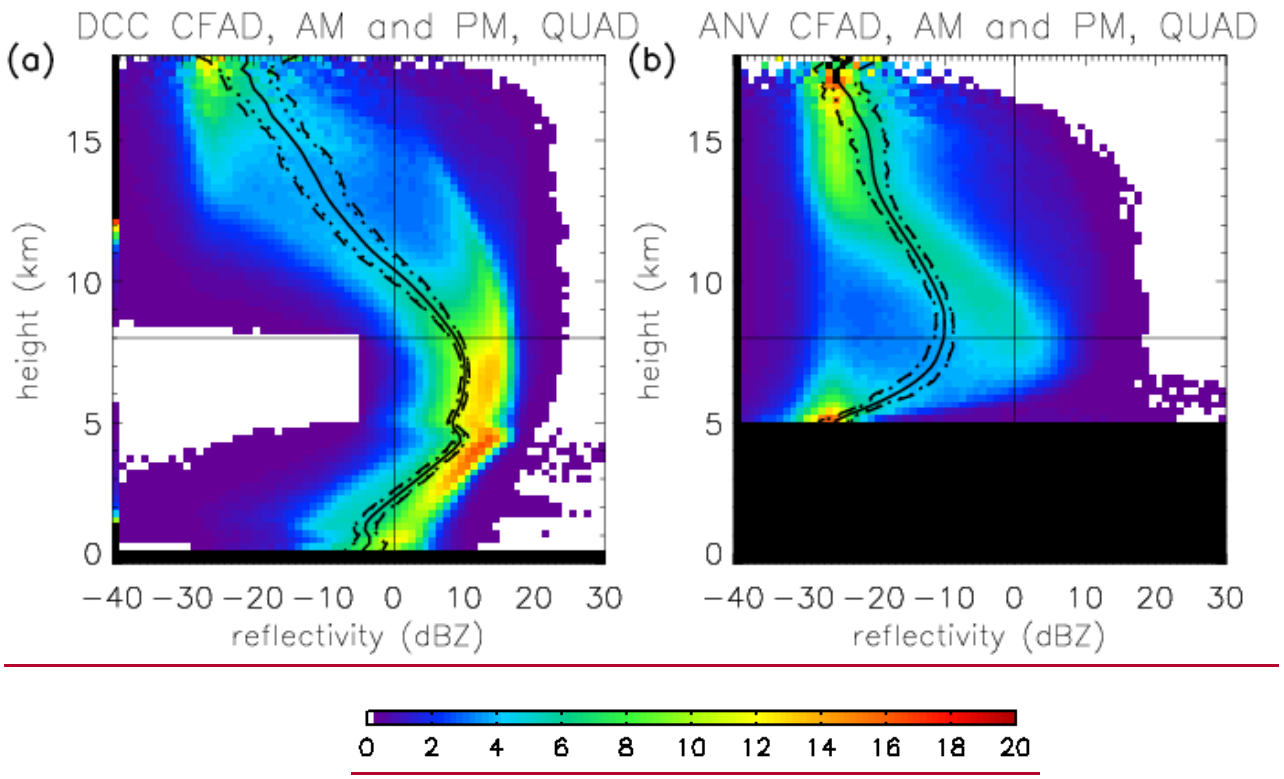

Figure 4. (a) The CFAD for DCCs, same as Fig. 3. The black curves near the center of the data are the average reflectivity profiles. Dashed lines are the standard deviation bounds. (b) Same as (a), but for anvils.

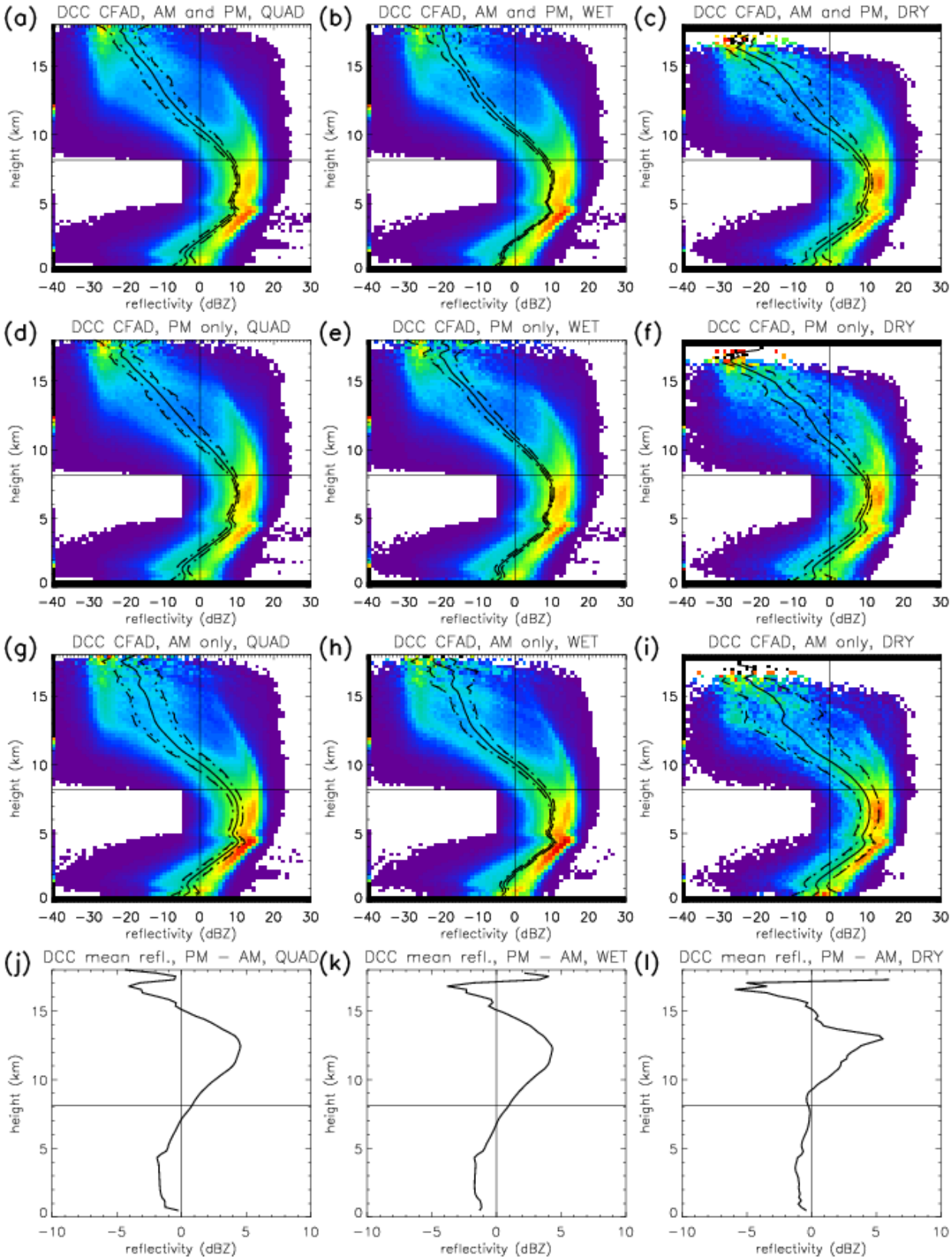

600

Figure 5. (a-i) The CFADs of reflectivity for DCCs in Amazonia separated by time of day and season. The left column is for all four seasons~~,~~ (wet, dry, wet-to-dry, and dry-to-wet), labelled QUAD; the middle column is for the wet season (DJF~~),~~); and the right column is the dry season (JJA). The first row are results for both times of day, the second row is day-only, and the third row is night-only.~~ The black curves near the center of the data are the average reflectivity profiles. Dashed lines are the standard deviation bounds. The vertical (horizontal) black line indicates 0 dBZ (8 km).~~

(j-l) The difference between the day and night mean reflectivity profile values – i.e, the second row minus the third row. ~~Dashed lines are the standard deviation.~~

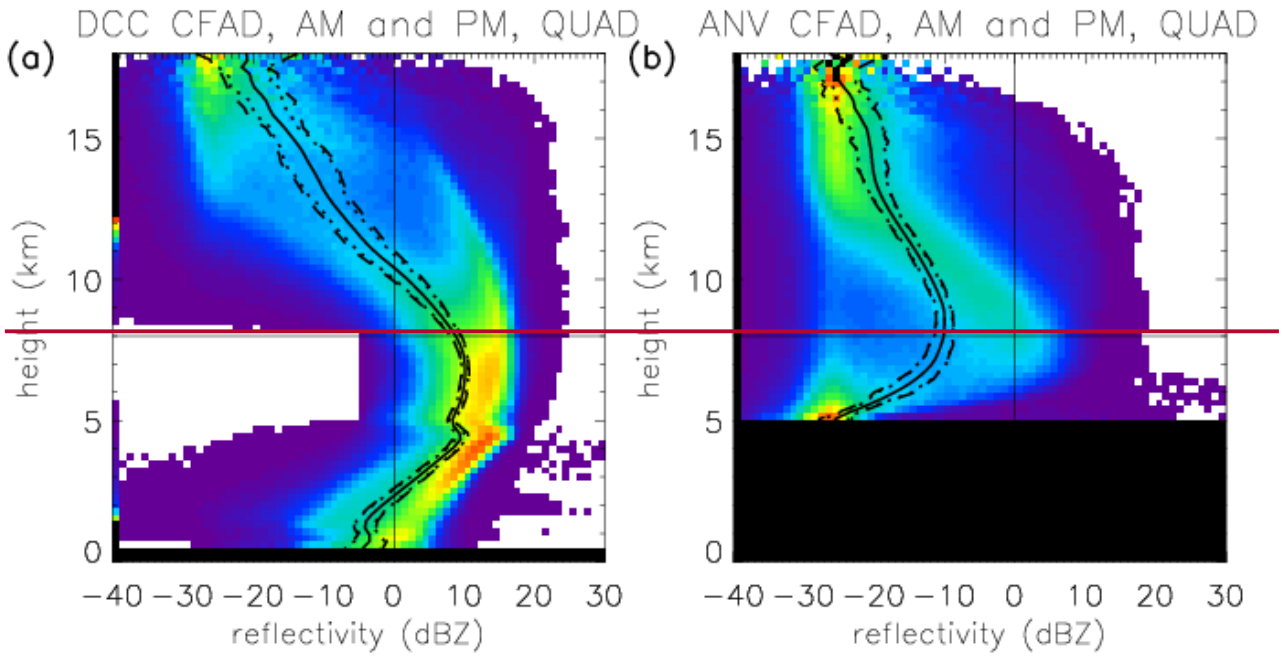

~~**Figure 4. (a) Same as Fig. 3a. (b) Same as (a), but for anvils.**~~

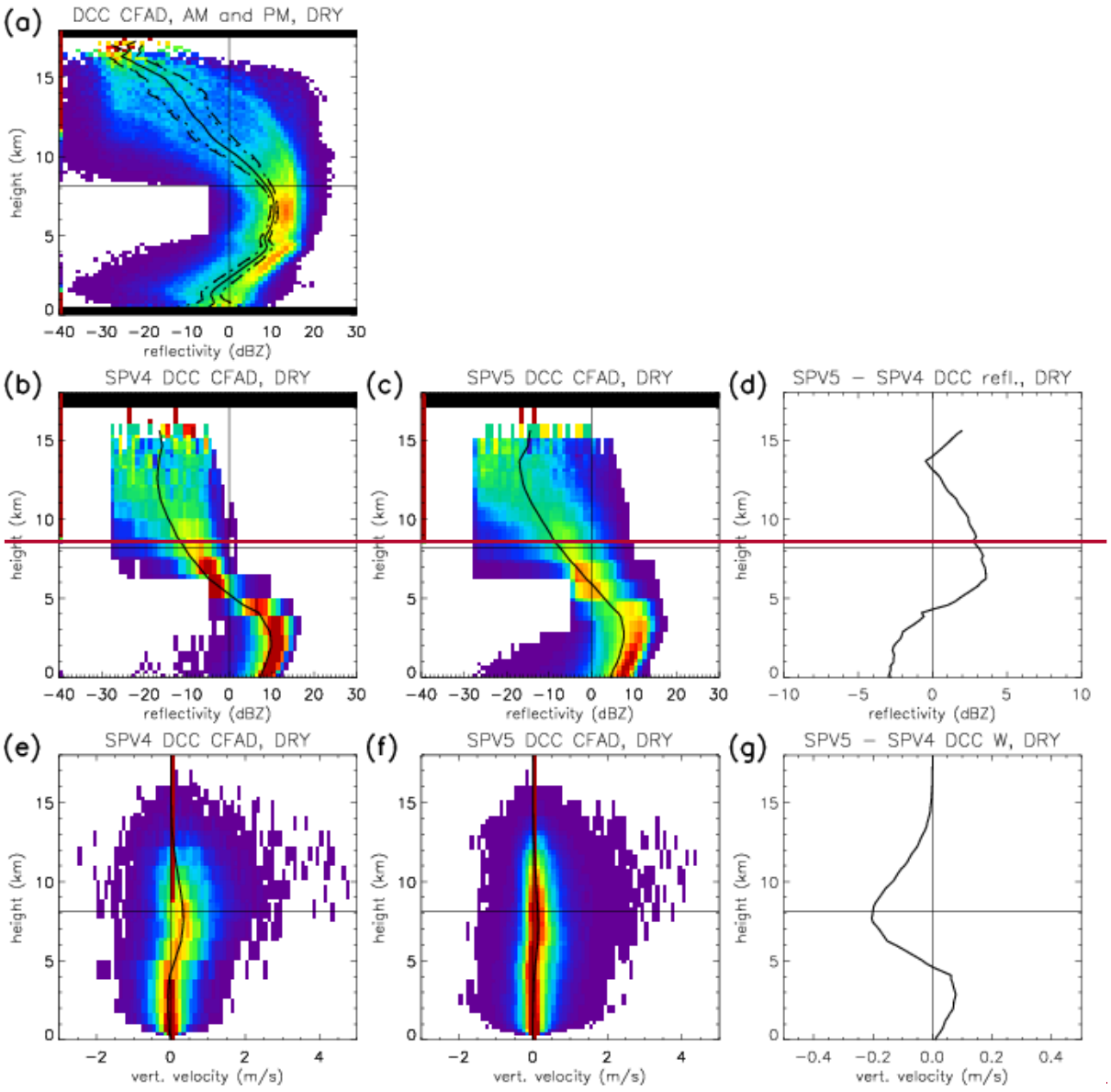
(a)
DCC CFAD, AM and PM, DRY
height (km)
reflectivity (dBZ)
(b)
SPV4 DCC CFAD, DRY
(c)
SPV5 DCC CFAD, DRY
(d)
SPV5 – SPV4 DCC refl., DRY
(e)
SPV4 DCC CFAD, DRY
vert. velocity (m/s)
(f)
SPV5 DCC CFAD, DRY
(g)
SPV5 – SPV4 DCC W, DRY

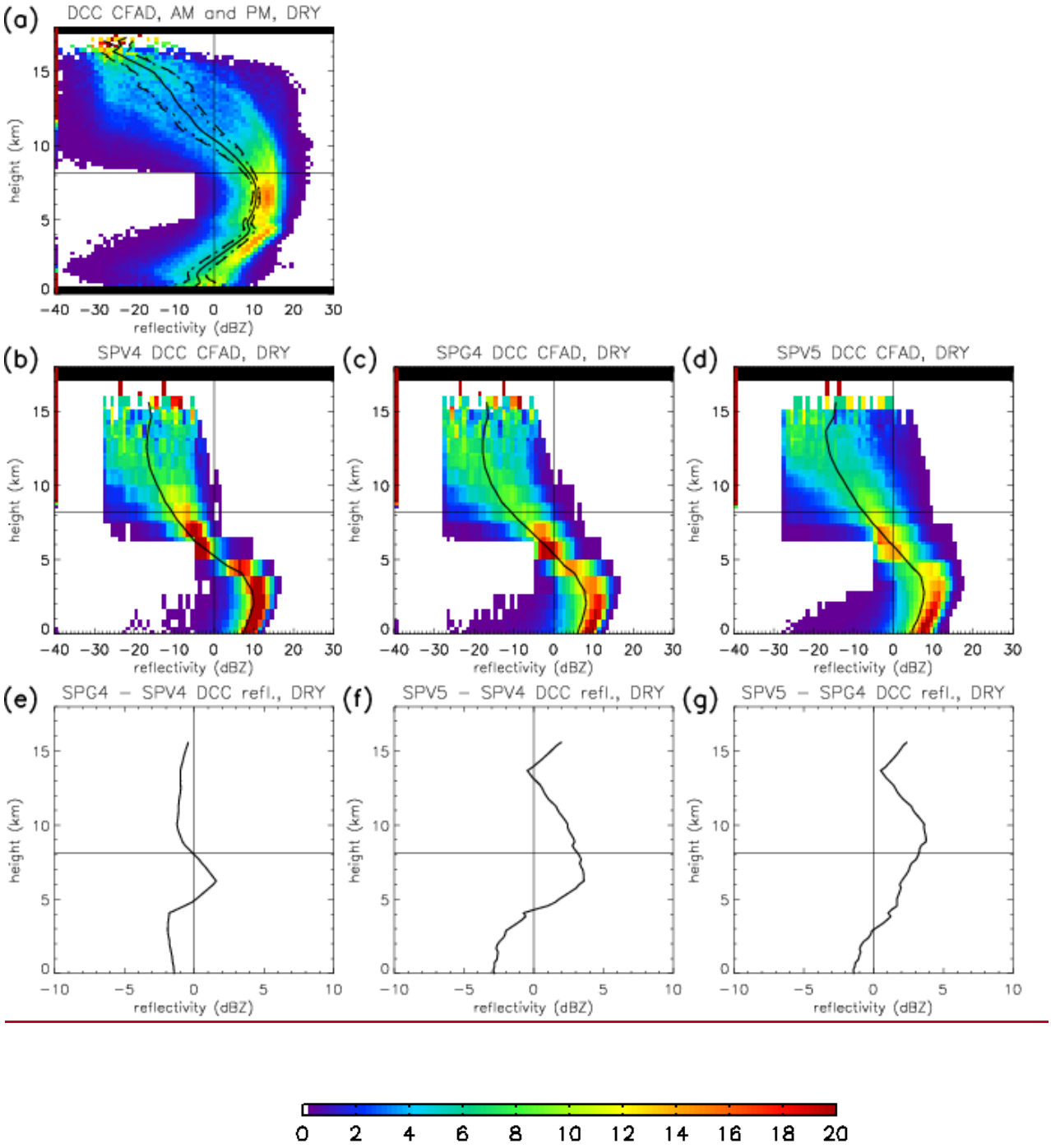

615

Figure ~~5~~6. (a,b,c,d) CFADs of dry season DCC reflectivity in Amazonia from (a) CloudSat, (b) SP-CAM version 4 ~~and~~, (c) SP-CAM version 4 with diagnosed graupel included, and (d) SP-CAM version 5, as in Fig. ~~3. (d~~4.

(e,f,g) The difference of the mean vertical reflectivity profile between ~~the~~(f) version 4 with diagnosed graupel and without, (f) version 5 and version 4, and (g) version 5 and version 4 with graupel.

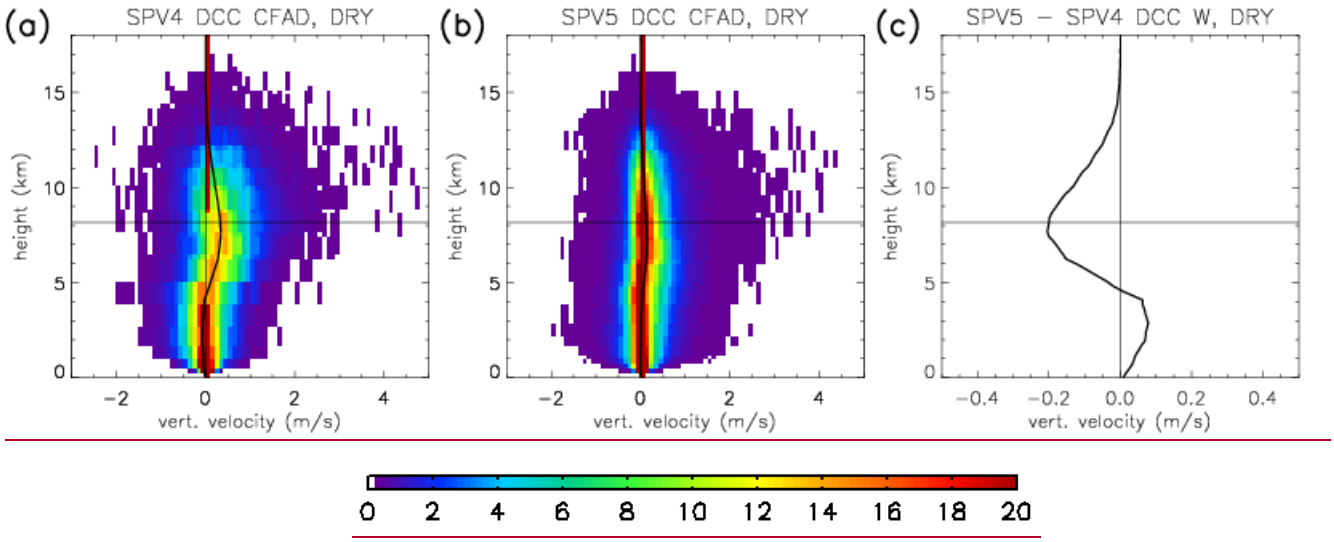

**Figure 7. ~~mean reflectivity profiles. (e,f~~(a,b) CFADs of DCC vertical updraft velocity from (ea) SP-CAM version 4 and (~~f~~b) SP-CAM version 5. The format is the same as for the reflectivity CFADs. ~~(g~~Note that SPV4 and SPG4 vertical velocities (not shown) are identical. (c) The difference between the version 4 and version 5 mean vertical velocity profiles.

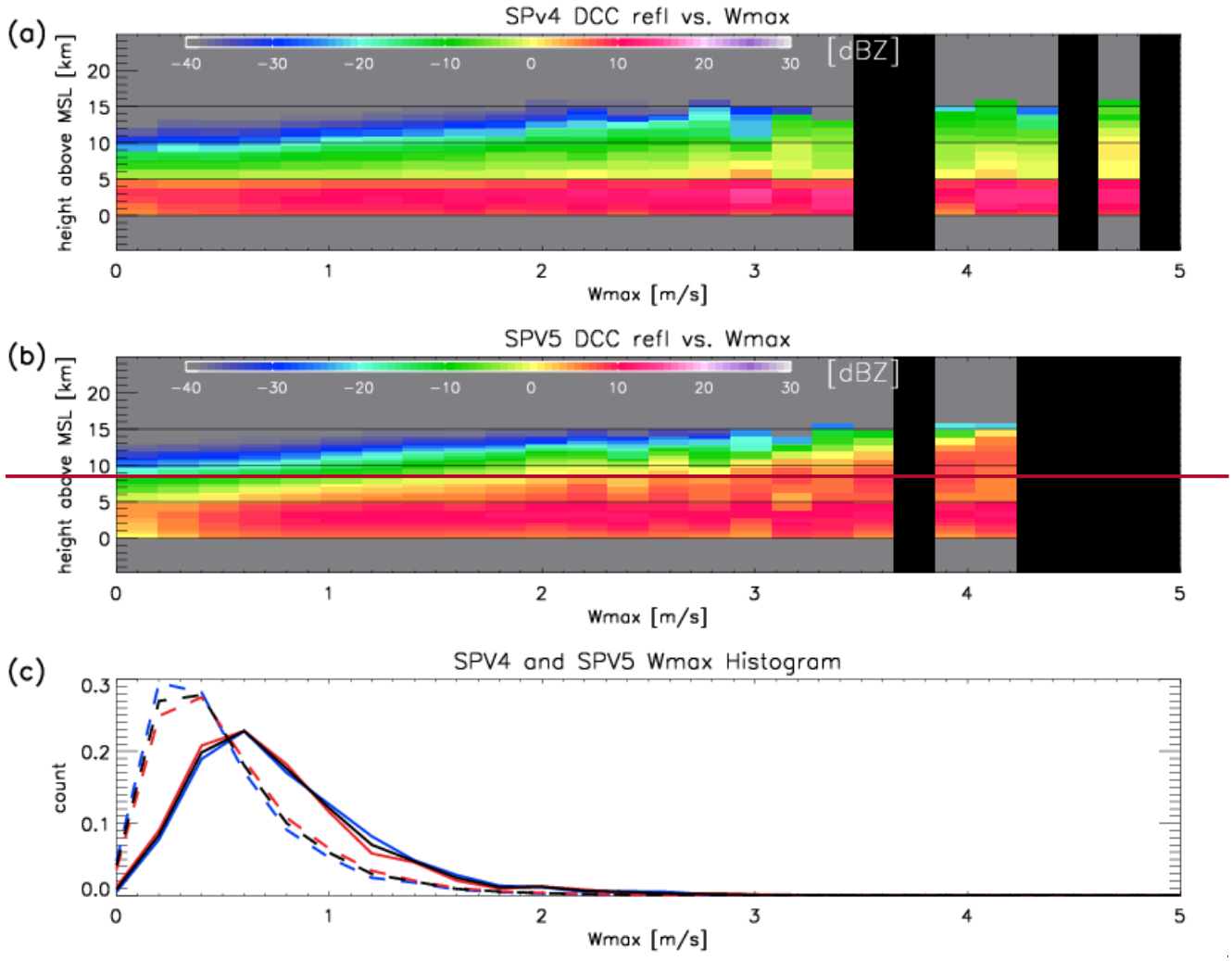

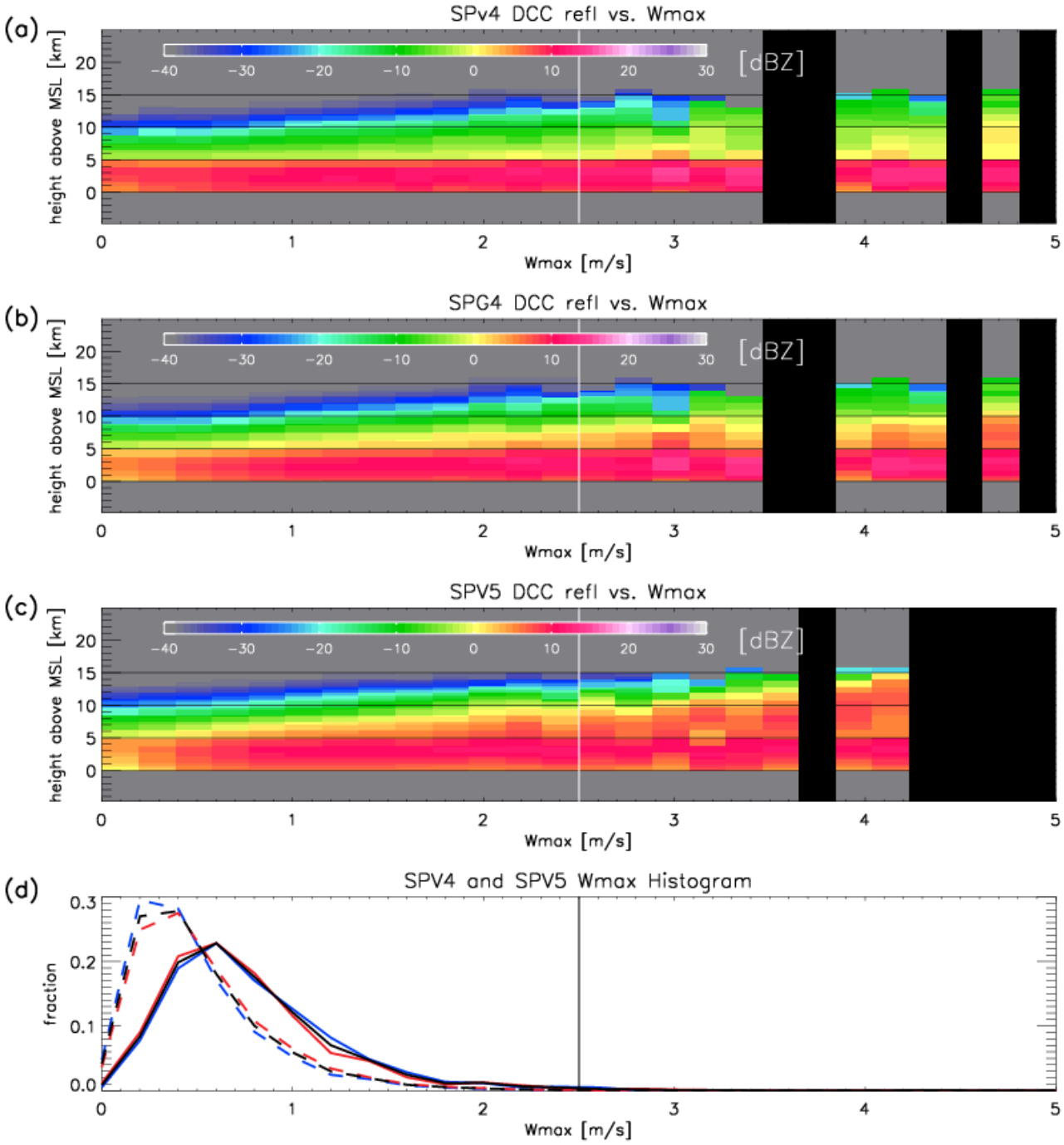

Figure ~~6~~8. (a) Mean vertical profiles of simulated DCC radar reflectivity in SPV4 sorted by maximum updraft velocity. The vertical lines at 2.5 m s^{-1} represent the maximum cut off W_{max} value for statistical calculations. Vertical black stripes are updraft values with no DCC occurrences.

(b) Same as (a), but for SPG4 data (i.e., SPV4 with diagnosed graupel included in the reflectivity calculation).

(c) Same as (a), but for SPV5 data.

(~~c~~d) PDFs of maximum DCC updraft velocity for (solid) SPV4 and (dashed) SPV5. The black line represents data from both 0200 and 1400 LST, the blue line from 0200 LST only (night), and the red line from 1400 LST only (day).

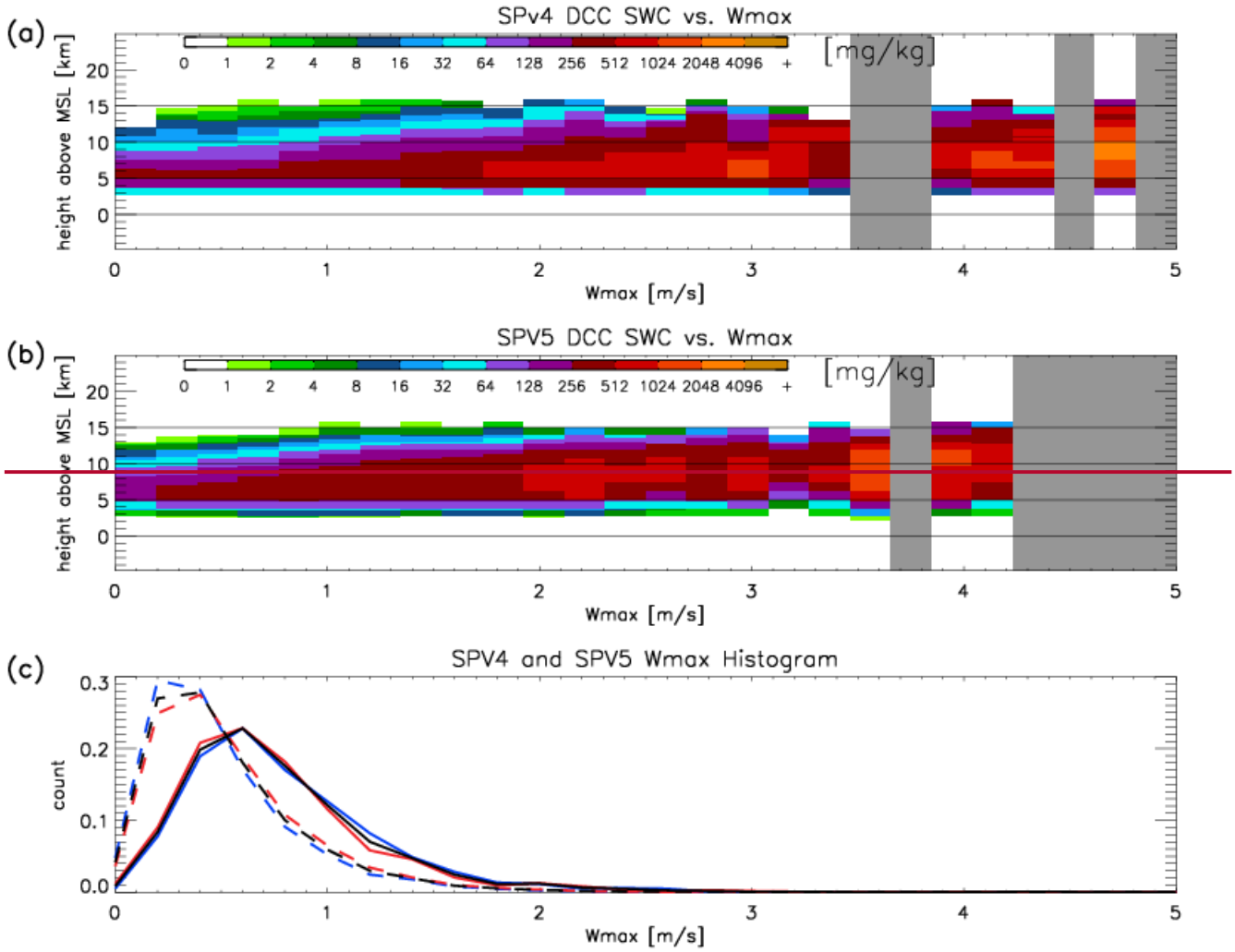
(a)
SPv4 DCC SWC vs. Wmax
0 1 2 4 8 16 32 64 128 256 512 1024 2048 4096 +
[mg/kg]
height above MSL [km]
Wmax [m/s]
(b)
SPV5 DCC SWC vs. Wmax
0 1 2 4 8 16 32 64 128 256 512 1024 2048 4096 +
[mg/kg]
height above MSL [km]
Wmax [m/s]
(c)
SPV4 and SPV5 Wmax Histogram
count
Wmax [m/s]

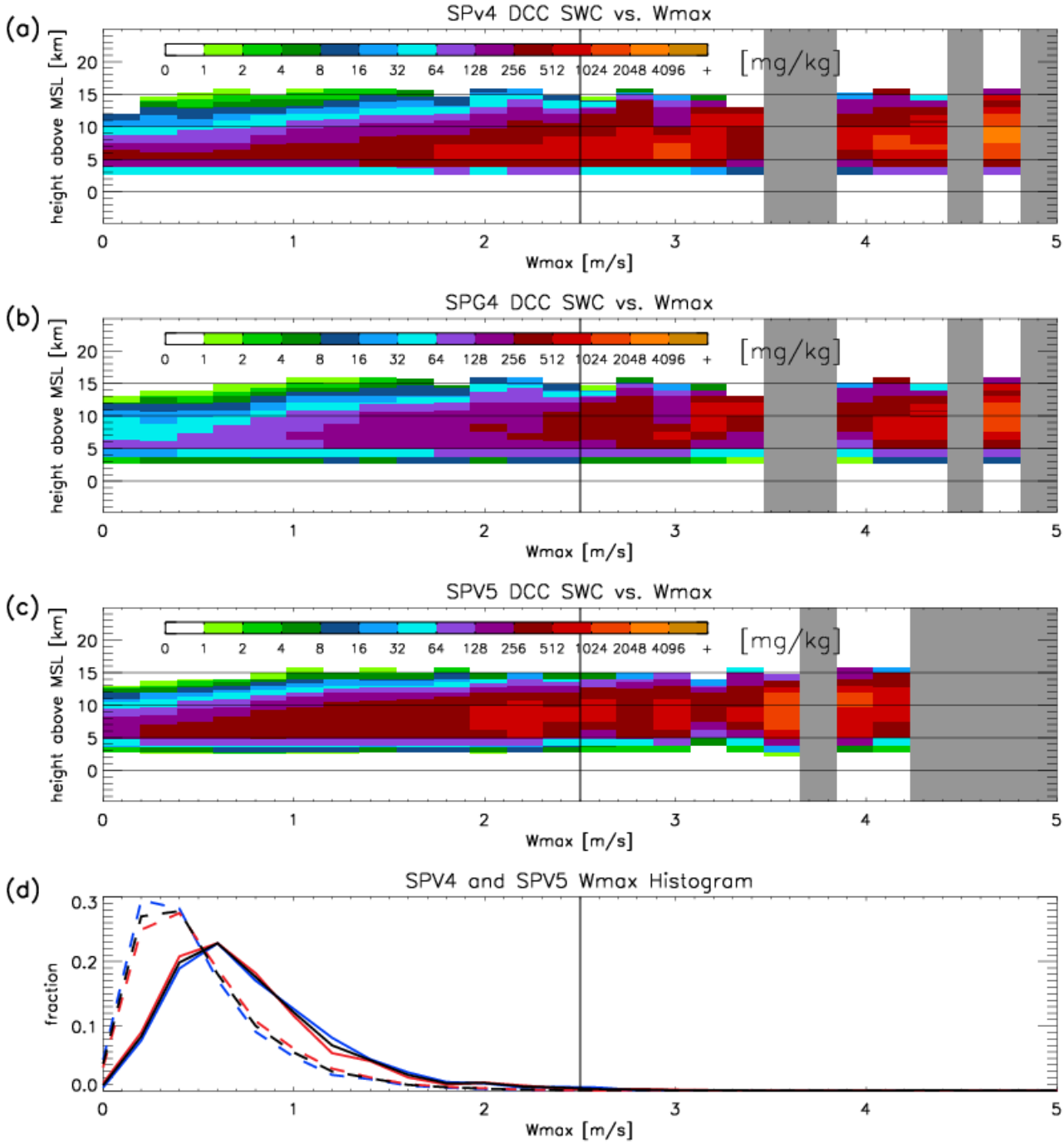

635

~~Figure 7. Same as Fig. 6~~Figure 9. Same as Fig. 8, but for snow water content (~~GWC).~~SWC). Because SPV4 does not distinguish between snow and graupel, all precipitating ice are depicted as SWC.

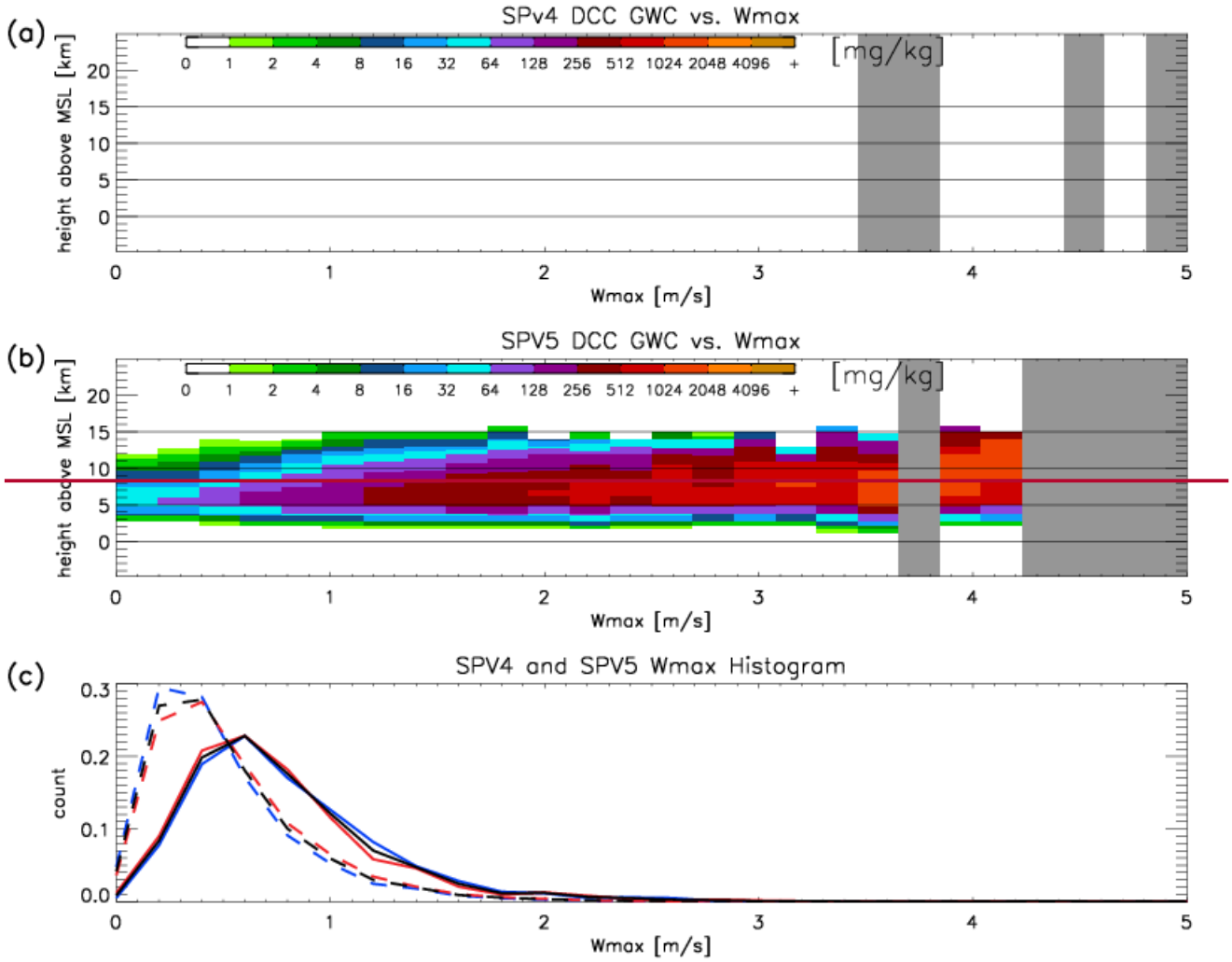
(a)
SPv4 DCC GWC vs. Wmax
0 1 2 4 8 16 32 64 128 256 512 1024 2048 4096 +
[mg/kg]
height above MSL [km]
Wmax [m/s]
(b)
SPV5 DCC GWC vs. Wmax
0 1 2 4 8 16 32 64 128 256 512 1024 2048 4096 +
[mg/kg]
height above MSL [km]
Wmax [m/s]
(c)
SPV4 and SPV5 Wmax Histogram
count
Wmax [m/s]

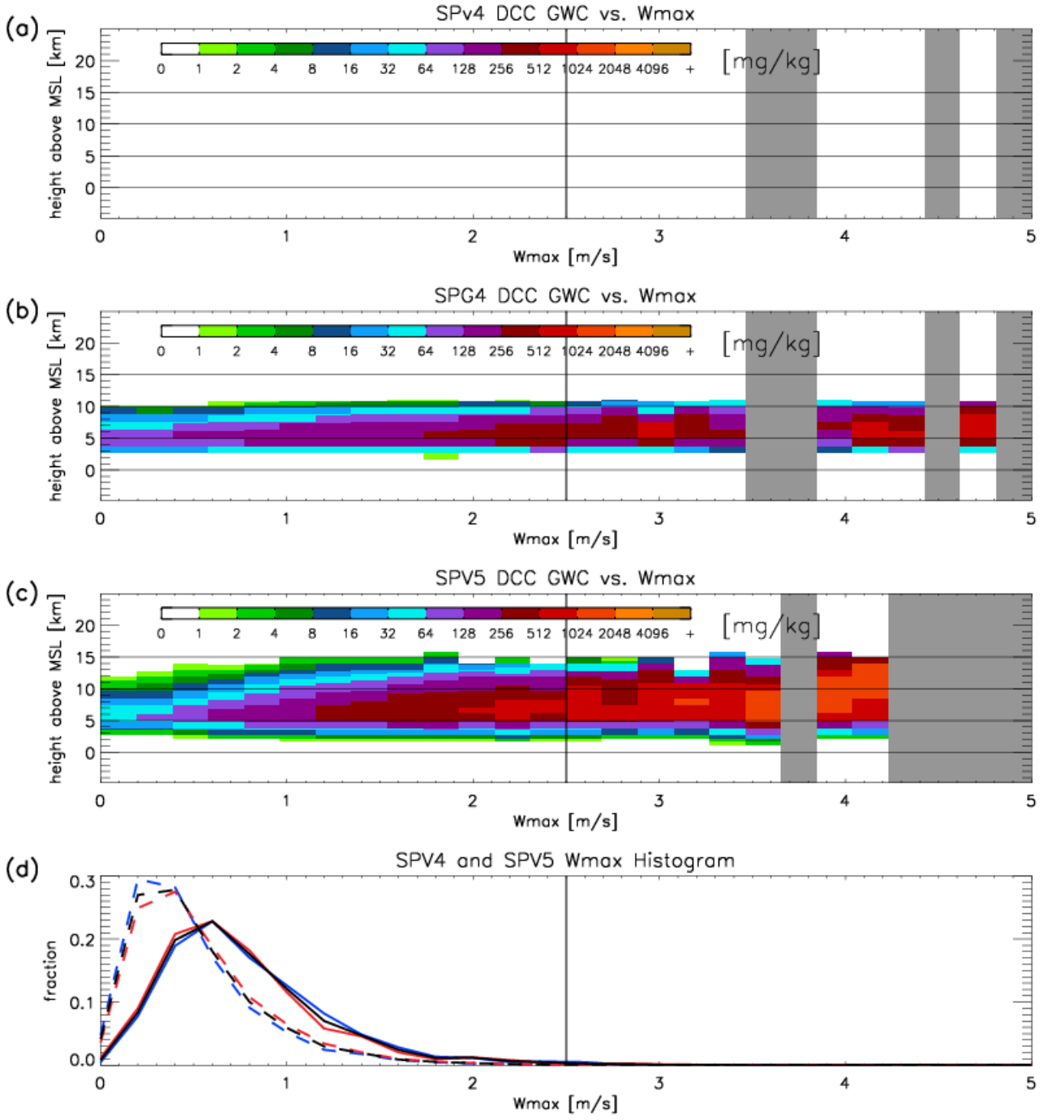

640 **Figure ~~8~~10. Same as Fig. ~~6~~8, but for graupel water content (GWC). Note the absence of GWC for SPV4.**

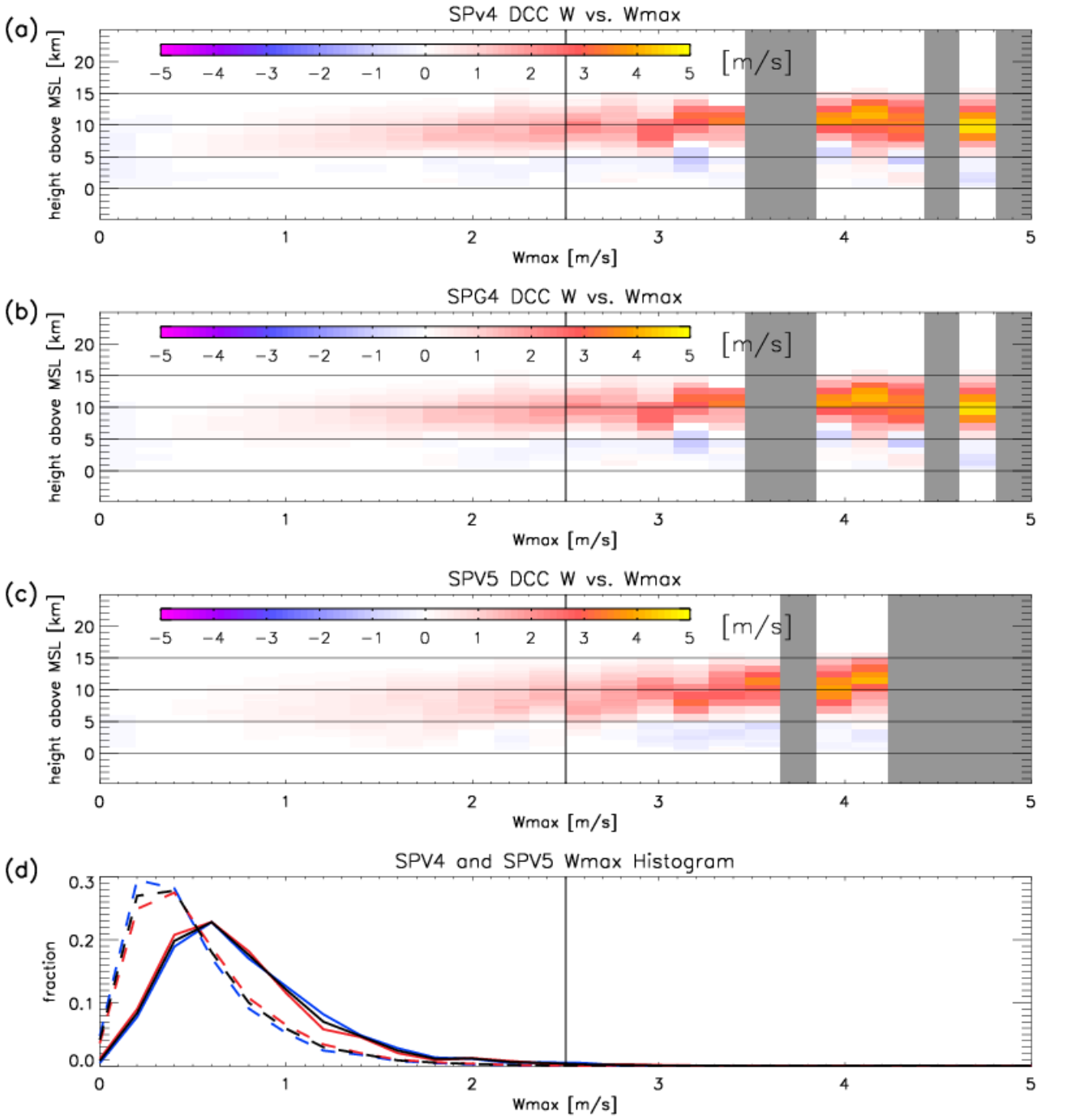
(a)
SPv4 DCC W vs. Wmax
[m/s]
height above MSL [km]
Wmax [m/s]
(b)
SPG4 DCC W vs. Wmax
[m/s]
height above MSL [km]
Wmax [m/s]
(c)
SPV5 DCC W vs. Wmax
[m/s]
height above MSL [km]
Wmax [m/s]
(d)
SPV4 and SPV5 Wmax Histogram
fraction
Wmax [m/s]

Figure 11. Same as Fig.

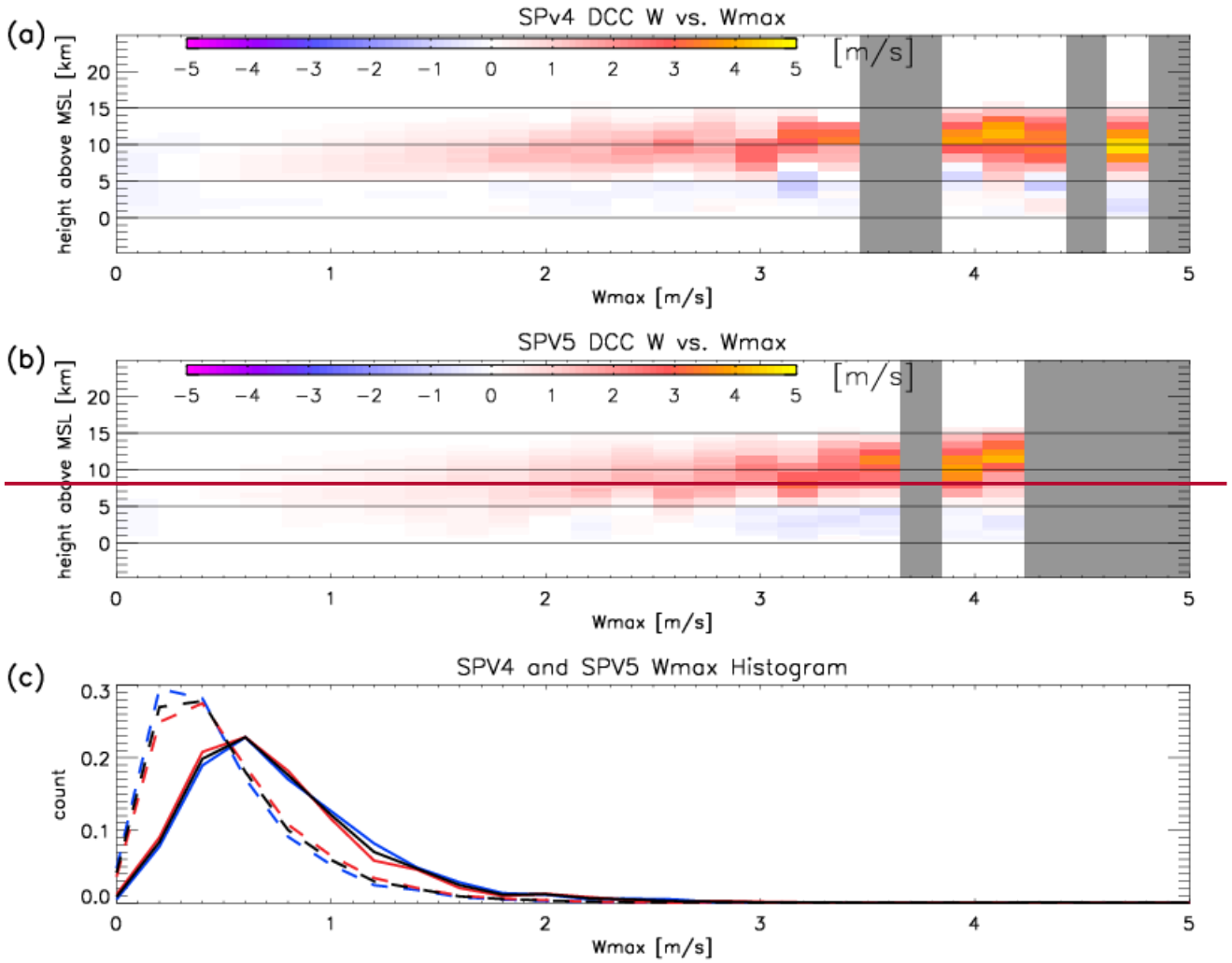

8~~Figure 9. Same as Fig. 6~~, but for DCC vertical velocity profiles. Note that the results for SPV4 and SPG4 are identical.